National Library of Canada
Acquisitions and Bibliographic Services Branch
395 Wellington Street
Ottawa, Ontario
K1A 0N4

Bibliothèque nationale du Canada
Direction des acquisitions et des services bibliographiques
395, rue Wellington
Ottawa (Ontario)
K1A 0N4

Your file Votre référence

Our file Notre référence

NOTICE

The quality of this microform is heavily dependent upon the quality of the original thesis submitted for microfilming. Every effort has been made to ensure the highest quality of reproduction possible.

If pages are missing, contact the university which granted the degree.

Some pages may have indistinct print especially if the original pages were typed with a poor typewriter ribbon or if the university sent us an inferior photocopy.

Reproduction in full or in part of this microform is governed by the Canadian Copyright Act, R.S.C. 1970, c. C-30, and subsequent amendments.

AVIS

La qualité de cette microforme dépend grandement de la qualité de la thèse soumise au microfilmage. Nous avons tout fait pour assurer une qualité supérieure de reproduction.

S'il manque des pages, veuillez communiquer avec l'université qui a conféré le grade.

La qualité d'impression de certaines pages peut laisser à désirer, surtout si les pages originales ont été dactylographiées à l'aide d'un ruban usé ou si l'université nous a fait parvenir une photocopie de qualité inférieure.

La reproduction, même partielle, de cette microforme est soumise à la Loi canadienne sur le droit d'auteur, SRC 1970, c. C-30, et ses amendements subséquents.

Canada

Adaptive Control of a Multizone Fan-Coil Heating System

Gurinder Singh

A Thesis

in

The Department

of

Electrical and Computer Engineering

Presented in Partial Fulfillment of the Requirements

for the Degree of Master of Applied Science at

Concordia University

Montréal, Québec, Canada

December 1993

© Gurinder Singh, 1993

National Library
of Canada

Acquisitions and
Bibliographic Services Branch

395 Wellington Street
Ottawa, Ontario
K1A 0N4

Bibliothèque nationale
du Canada

Direction des acquisitions et
des services bibliographiques

395, rue Wellington
Ottawa (Ontario)
K1A 0N4

Your file Votre référence

Our file Notre référence

The author has granted an irrevocable non-exclusive licence allowing the National Library of Canada to reproduce, loan, distribute or sell copies of his/her thesis by any means and in any form or format, making this thesis available to interested persons.

L'auteur a accordé une licence irrévocable et non exclusive permettant à la Bibliothèque nationale du Canada de reproduire, prêter, distribuer ou vendre des copies de sa thèse de quelque manière et sous quelque forme que ce soit pour mettre des exemplaires de cette thèse à la disposition des personnes intéressées.

The author retains ownership of the copyright in his/her thesis. Neither the thesis nor substantial extracts from it may be printed or otherwise reproduced without his/her permission.

L'auteur conserve la propriété du droit d'auteur qui protège sa thèse. Ni la thèse ni des extraits substantiels de celle-ci ne doivent être imprimés ou autrement reproduits sans son autorisation.

ISBN 0-315-90890-4

Canada

ABSTRACT

Adaptive Control of a Multizone Fan-Coil Heating System

Gurinder Singh

The application of adaptive control to a multizone fan-coil heating (MFCH) system is studied. A two-zone fan-coil heating system is considered. The system consists of two-zones, a fan-coil unit for each zone, a boiler, and distribution piping. A nonlinear model of the two-zone fan-coil heating system is developed. The thermal dynamic effect of the enclosure elements is described by two fifth-order models, one for each zone. The environmental zones are acted upon by multiple disturbances such as changes in outdoor temperature, solar radiation fluxes, and dynamic disturbances due to the thermal inertia of the enclosure elements.

An adaptive controller is designed using pole placement and LQR theory. A proof of stability of the closed-loop system is given. Simulation results showing the closed-loop response of the system to changes in operating points, external disturbances, changes in system parameters, and unmodeled dynamics are presented.

It is shown that the adaptive controller is able to adapt to a wide range of operating conditions and maintain the zone and boiler temperatures close to their respective setpoints.

ACKNOWLEDGEMENTS

I would like to express my gratitude and due appreciation for my supervisors Dr. R. V. Patel and Dr. M. Zaheeruddin for initiating this project, and their guidance and encouragement in all phases of this research work. I wish to thank Dr. Salem Al-Assadi for his numerous suggestions throughout this research work. And finally, special thanks and appreciation are due to my family and friends for their encouragement and moral support.

TABLE OF CONTENTS

LIST OF FIGURES vii

LIST OF TABLES x

LIST OF SYMBOLS xi

1 Introduction **1**

1.1 General 1

1.2 Introduction to Adaptive Control 2

1.3 PID Control for HVAC Systems 6

1.4 Summary 9

2 Literature Survey **11**

2.1 Introduction 11

2.2 Adaptive Control for HVAC Systems: A Survey 12

2.3 Objectives of the Thesis 19

3 Modeling and Controller Design **20**

3.1 Introduction 20

3.2 Physical Model 21

3.3 Analytical Model 23

3.4 Open-Loop Simulation Results 28

3.5 Controller Design 32

3.5.1 Problem Statement 34

3.5.2 Controller Structure 37

3.5.3 Pole Placement Problem 41

3.5.4 LQR Problem 42
3.6 Summary 43

4 Stability and Implementation 45

4.1 Introduction 45
4.2 Stability 46
4.2.1 Lyapunov's Stability Criterion 46
4.3 Implementation 48
4.4 Summary 51

5 Results and Discussion 55

5.1 Introduction 55
5.2 Effects of Step Changes in Initial Conditions and Disturbances 56
5.3 Robustness 66
5.4 Effect of Introducing Estimation-Error Feedback 70
5.5 Effect of Adding Extra Dynamics 79
5.6 Comparison of Adaptive Controller with Fixed-Gain Controller 81

6 Conclusions and Extensions 86

References 89

LIST OF FIGURES

1.1 A nonlinear feedback system. 10

3.1 Schematic diagram of a multi-zone fan-coil heating (MFCH) system. . 22

3.2 Open-loop response of the MFCH system. 29

3.3 Effect of step changes in the control input on the open-loop response of the MFCH system. 30

3.4 Open-loop response of the system when the initial conditions are perturbed by 1.0 deg C. 31

3.5 A robust controller for the servomechanism problem 38

4.1 Overall configuration of the robust controller for the servomechanism problem 52

5.1 Closed-loop response showing the effect of perturbations in the initial conditions for the controller designed using pole placement theory . . 58

5.2 Closed-loop response showing the effect of perturbations in the initial conditions for the controller designed using LQR theory. 60

5.3 Closed-loop response showing the effect of perturbations in initial conditions and static disturbance for the controller designed using pole placement theory 61

5.4 Closed-loop response showing the effect of perturbations in initial conditions and static disturbance for the controller designed using LQR theory. 62

5.5 Closed-loop response showing the effect of perturbations in initial conditions and static disturbances for the controller designed using pole placement theory: Improved response. 64

5.6 Closed-loop response showing the effect of perturbation in initial conditions, static, and dynamic disturbances for the controller designed using pole placement theory 65

5.7 Closed-loop response showing the effect of perturbations in initial conditions, static, and dynamic disturbances for the controller designed using LQR theory. 67

5.8 Closed-loop response showing the effect of perturbation in initial conditions and dynamic disturbance for the controller designed using pole placement theory 68

5.9 Closed-loop response showing the effect of perturbations in initial conditions and dynamic disturbance for the controller designed using LQR theory. 69

5.10 Closed-loop response showing the robustness properties when the controller is designed using pole placement theory: a_{z1} is changed by 30 % 71

5.11 Closed-loop response showing the robustness properties when the controller is designed using pole placement theory: a_{z1} and a_{z2} are changed by 30 % each. 72

5.12 Closed-loop response showing the robustness properties when the controller is designed using pole placement theory: ξ_z is changed by 20 % 73

5.13 Closed-loop response showing the robustness properties w .en the controller is designed using pole placement theory: a_{z1}, a_{z2}, and ξ_z are changed by 30 %, 30 %, and 20 % respectively. 74

5.14 Closed-loop re.ponse showing the robustness properties when the controller is designed using LQR theory: a_{z1} is changed by 30 % 75

5.15 Closed-loop response showing the robustness properties when the controller is designed using LQR theory: a_{z1} and a_{z2} are changed by 30 % each. 76

5.16 Closed-loop response showing the robustness properties when the controller is designed using LQR theory: ξ_z is changed by 20 %. 77

5.17 Closed-loop response showing the robustness properties when the controller is designed using LQR theory: a_{z1}, a_{z2}, and ξ_z are changed by 30 %, 30 %, and 20 % respectively. 78

5.18 Closed-loop response when there is no estimation-error feedback to the controller. 80

5.19 Closed-loop response showing the effect of adding extra valve dynamics when the controller is designed using pole placement. 82

5.20 Closed-loop response showing the effect of adding extra valve dynamics when the controller is designed using LQR. 83

5.21 Closed-loop response showing the effect of step changes in the operating point with adaptive controller. 84

5.22 Closed-loop response showing the effect of step changes in the operating point with fixed-gain controller. 85

LIST OF TABLES

3.1 List of symbols with their nominal values. 38

4.1 List of symbolic representation of the variables and their sizes . . . 54

LIST OF SYMBOLS

A_{d_1}	Surface area of enclosure walls for zone 1
A_{d_2}	Surface area of enclosure walls for zone 2
C1	Control valve for zone 1
C2	Control valve for zone 2
C3	Control valve for boiler
C_{z1}	Thermal capacity of air in zone 1
C_{z2}	Thermal capacity of air in zone 2
C_b	Boiler thermal capacity
DDC	Direct digital controller
K_d	Derivative gain
K_i	Integral gain
K_p	Proportional gain
K_1, K_2, K_3	Gain Matrices
M_d	Amplitude of the sinusoidal disturbance
M_r	Amplitude of the sinusoidal reference signal
T_a	Outdoor temperature
T_b	Temperature of boiler
$T_{b_{max}}$	Maximum temperature of the boiler
$\mathbf{T_{d_1}}$	State of dynamic disturbance model for zone 1
$T_{d_{11}}$	Dynamic disturbance for zone 1
$T_{d_{12}}$	Dynamic disturbance for zone 2
$\mathbf{T_{d_2}}$	State of dynamic disturbance model for zone 2
T_p	Boiler room temperature

T_{z1}	Temperature of zone 1
T_{z2}	Temperature of zone 2
V_p	Output of the controller
a_b	Heat loss coefficient of boiler surfaces
a_{z1}	Heat loss coefficient of zone 1
a_{z12}	Inter zone heat loss coefficient
a_{z2}	Heat loss coefficient of zone 2
$\mathbf{d_d}$	Dynamic disturbance vector
$\mathbf{d_s}$	Static disturbance
$\mathbf{e}$	Output error vector
$\mathbf{e_s}$	Estimation error
h	Heat transfer coefficient between interior wall to the room air
$\mathbf{u}$	Control input vector
u_1	Normalized mass flow rate of hot water through control valve C1
u_2	Normalized mass flow rate of hot water through control valve C2
u_3	Normalized mass flow rate of natural gas through control valve C3
$u_{1_{max}}$	Maximum mass flow rate of water through valve 1
$u_{2_{max}}$	Maximum mass flow rate of water through valve 2
$u_{3_{max}}$	Maximum capacity of burner
u_{m1}	Mass flow rate of hot water through control valve C1
u_{m2}	Mass flow rate of hot water through control valve C2
u_{m3}	Mass flow rate of natural gas through control valve C3
w	Solar heat gain
$\mathbf{x}$	State vector of the actual nonlinear MFCH system

α	Boiler fuel loss parameter
ξ_z	Heat transfer coefficient
$\Delta\xi$	Output of the servocompensator

Chapter 1

Introduction

1.1 General

Designing good control strategies for the operation of a Heating, Ventilating, and Air-Conditioning (HVAC) system are most important from the viewpoint of saving energy and improving human comfort in indoor environmental spaces. This problem is very challenging because even simple HVAC systems are nonlinear and there exists a strong coupling between the zone models, fan-coil models, and boiler model. In this thesis, a system's approach is used to design controllers for an HVAC system.

Since a central HVAC system consists of several subsystems, the control system must coordinate the operation of the subsystems to produce the desired outputs. In this sense, more than one control input is to be regulated to hold the outputs at the desired levels.

In this study, we have used adaptive gains derived from linear control theory to control the nonlinear multi-input multi-output (MIMO) multi-zone fan-coil heating (MFCH) system. It is very hard to represent the MFCH system exactly by a

nonlinear dynamical model because there are some dynamics which cannot be modeled exactly such as valve dynamics, damper dynamics etc. There may also be some dynamical units of the plant whose operation will deteriorate after some time and as such analytical models of those units will not represent them exactly. If we use these analytical models to design control strategies, the system's performance may not be satisfactory. During the operation of the plant, if we want to include some dynamical components into the plant, even then we have to re-compute the control laws. To overcome these uncertainties in the model dynamics, we use adaptive gains which will compensate for all unmodeled dynamics. Even if the environment in which the system is working changes, adaptive gains will attempt to adapt themselves to make the system performance satisfactory.

1.2 Introduction to Adaptive Control

One of the fundamental principles of modern control theory is that a plant cannot be well controlled until it can be modeled in quantitative terms, and its states are observed or reconstructed in a deterministic or stochastic sense. This has resulted in such notions as identification, parameter and state estimation, filtering and observers. One of fundamental implicit concerns in the field of control theory is the notion of "learning and self-adaptive control". Using some of these concepts and notions the field of adaptive control has evolved over the past three decades from primitive hill-climbing methods to advanced adaptive control techniques.

Today, adaptive control has potential applications for control of almost all technological systems in which the inherent complexities associated with explicit

identification and parameter estimation do not permit the applications of conventional control tools. It is a fascinating field for research. The word "adapt" means to change the behavior of a system to conform to new conditions. The adaptive control field has matured due to research in recent years, and a wide spectrum of problems has emerged. Intuitively, an adaptive controller is a controller that can modify its behavior according to changes in the dynamics of a process and disturbances acting on it [1]. In contrast to conventional control, adaptive control refers to the control of partially known systems. The characteristics of the process can be time varying due to a variety of reasons. There may be changes in the environment such as unforeseen changes in the statistics of external inputs and disturbances acting on the system. The use of conventional control theory will not give satisfactory response under time-varying conditions [2]. As is well known *feedback* was also introduced to give satisfactory response when there are parameter variations by increasing the loop gain of the system [4]. The main drawback of the *high-gain* controllers is that the magnitude of control signal may become large which could ultimately saturate the control inputs and cause instability.

Drenick and Shabender [3] introduced the term *adaptive system* in control theory to represent control systems that monitor their own performance and adjust their parameters in the direction of better performance. By viewing different characteristics of systems, different control actions were planned and hence different control systems were designed. This resulted in a profusion of definitions, each containing some property that its proponent considered peculiar to adaptive systems.

Aseltine et al. [5] has categorized adaptive systems into the following four classes depending on the manner in which adaptation takes place:

1. Passive adaptation.

2. Input-output adaptation.

3. System-variable adaptation.

4. System-characteristic adaptation.

Although these techniques are not commonly used these days, they are nevertheless of historical interest because research in adaptive control has led to similar ideas. A brief summary of the above mentioned adaptation methods is as follows.

Passive adaptation

It results in those systems in which the clever design of a time-invariant controller results in satisfactory performance over wide variations in the environment. An example of passive adaptation is given in Figure 1.1. The damping characteristics of a second-order servomechanism problem are improved by nonlinear feedback. The overall system shown in Figure 1.1 can be described by a nonlinear scalar differential equation of the form

$$\frac{d^2x}{dt} + (a + bx)\frac{dx}{dt} + cx = u \tag{1.1}$$

Although the system in (1.1) is nonlinear, the aim here is to determine a controller of fixed structure and known parameters to improve its performance. According to present usage, such controller would be described as *robust* rather than adaptive.

Input-output adaptation

In this adaptation scheme, input signal characteristics are used to adjust the parameters of the controller. The assumption here is that the performance of the overall system depends on some characteristics of the signal and that the optimal parameter values can be determined once these characteristics are known. Automatic gain

control systems can be considered as using this type of adaptation scheme. In these systems, a gain parameter is adjusted to maintain the average output amplitude constant when there are large variations in the amplitude of input signals. Assuming that optimal parameter values have been computed off-line for each class of input signals, they can be chosen on-line by referring to a look-up table. This method is called *gain scheduling*. Gain scheduling has been employed successfully in a variety of applications including process control and control of aircraft systems.

System-variable adaptation

In this adaptation scheme, the control input is adjusted based on the measurements of the system variables while the system is in operation. For example, the control input is adjusted based on variables such as system outputs, tracking errors and/or their derivatives, which can be measured.

System-characteristics adaptation

Adjustment of the control parameters or control input is done based on system characteristics, such as its impulse response or step response, or frequency response. For example, from the measured impulse response of a given plant, the damping ratio can be computed which can then be used to generate a feedback control signal.

More than two decades after the term *adaptation* was introduced, the definition of an adaptive system continues to be multifaceted and cannot be compressed into a single statement without loss of vital content. Different researchers have tried to define adaptive control in different ways, out of which the following definitions have largely evolved [6], [7]:

Definition 1.1 An adaptive system is one which is provided with a means of continuously monitoring its own performance in relation to a given figure of merit or optimal condition and a means of modifying its own parameters by a closed-loop action so as to approach this action.

Definition 1.2 An adaptive control system is defined as a feedback control system that is intelligent enough to adjust its characteristics in a changing environment so as to operate in an optimum manner according to some specified criterion.

Definition 1.3 An adaptive control system is one that is defined from an adaptive viewpoint.

The definitions cited above reveal that not only a variety of personal visions of adaptation are encountered in the field, but also that feedback together with estimation and control is an integral part of an adaptive control strategy. The complexity of adaptation increases as a parameter in an existing system is adjusted to cope with a new uncertainty, and hence becomes a state variable at the next level. According to Zadeh [8], any system can be defined as being adaptive by the proper choice of the uncertainty and the acceptance level of performance.

1.3 PID Control for HVAC Systems

HVAC systems waste energy and do not provide a comfortable environment if they are not controlled properly and are not well maintained [9]. This energy waste is primarily due to several undetected malfunctions in HVAC control systems. Detection of these malfunctions require skilled manpower for operation and maintenance. Furthermore, a high priority is given to the initial cost of control systems which results in poor performance of control components due to lack of quality.

To maintain space comfort conditions, HVAC control systems have mainly used feedback control in conjunction with thermostatic sensing devices [10]. Typically the proportional control action is taken on the output error. Such proportional control action is described as

$$V_p = K_p e \tag{1.2}$$

where

V_p = output of the proportional controller

K_p = proportional gain

e = error signal or offset

The drawback of this control scheme is that the HVAC system's output and space temperature continually oscillate above and below their setpoints because of lag times between the space, sensor, and the system response. This offset causes system inefficiency when steady state operating conditions are much needed.

To reduce the offset, proportional, integral, and derivative (PID) control sequencing is used. The mathematical representation of this control scheme is given by

$$V_p = K_p e + K_i \int e dt + K_d \frac{de}{dt} \tag{1.3}$$

where

V_p = output of the PID controller

K_p = proportional gain

e = error signal or offset

K_i = integral gain

t = time

K_d = derivative gain of the controller

This control action results in faster response and greater stability than simple proportional controls [11].

Although PID control reduces or eliminates offset, improper selection of proportional and integral gains can cause system instability. Also the derivative term may cause the controller to be very sensitive to noisy signals. HVAC systems comprise of a large number of subsystems, each of which may exhibit time-varying and/or nonlinear characteristics [12]. For example, a detailed mathematical description of a five-zone commercial HVAC system requires about 1000 differential and algebraic equations. Furthermore, the parameters of HVAC systems generally vary with load, weather, and building occupancy. In these situations, PI or PID control techniques do not give satisfactory performance [13]. The need for an alternative to classical fixed gain PI or PID control in those loops where the dynamical characterization of the components (sensor, coil etc.) vary significantly during operation was identified as a main reason for adaptive control [14].

There are a number of advantages in using adaptive controllers in HVAC systems. Commissioning costs would be less since the commissioning period would be shorter and the procedure would demand the attention of less skilled personnel. Since adaptive controllers might be better able to cope with nonlinear, dynamic behavior of the plant, it would be possible to simplify the control scheme and reduce installation costs by eliminating some of the cascaded control loops. The overall performance of the controllers would be better than that of conventional controllers since they would be able to adapt to the long-term, seasonal changes in the operation of the plant, thus improving comfort control, lowering energy consumption, and reducing maintenance costs.

Motivated by these considerations, we are interested, in this thesis, in exploring the design of a multivariable adaptive controller for a multi-zone fan-coil heating system (MFCH) system. To this end, this thesis is divided into six chapters. In the first chapter, an introduction to an adaptive control is given. The disadvantages of using constant-gain controllers in HVAC systems and the advantages of using adaptive controllers are also discussed. In Chapter 2, a review of the previous work on adaptive control implementation in HVAC systems is given, and the objectives of the proposed research are outlined. Physical and analytical models are described in Chapter 3. Open-loop response of the MFCH system is studied and controller design techniques using robust servomechanism principles, are explained. Stability which is a basic requirement in any control system, is discussed in Chapter 4. This is followed by a discussion of implementation issues of the robust controller for the MFCH system. Simulation results for various operating conditions are given in Chapter 5. Conclusions and suggestions for further work are given in Chapter 6.

1.4 Summary

In this chapter, a brief introduction to adaptive control has been given. The reasons for the ineffectiveness of PI and PID controllers, and the advantages of using adaptive control for HVAC systems are also outlined.

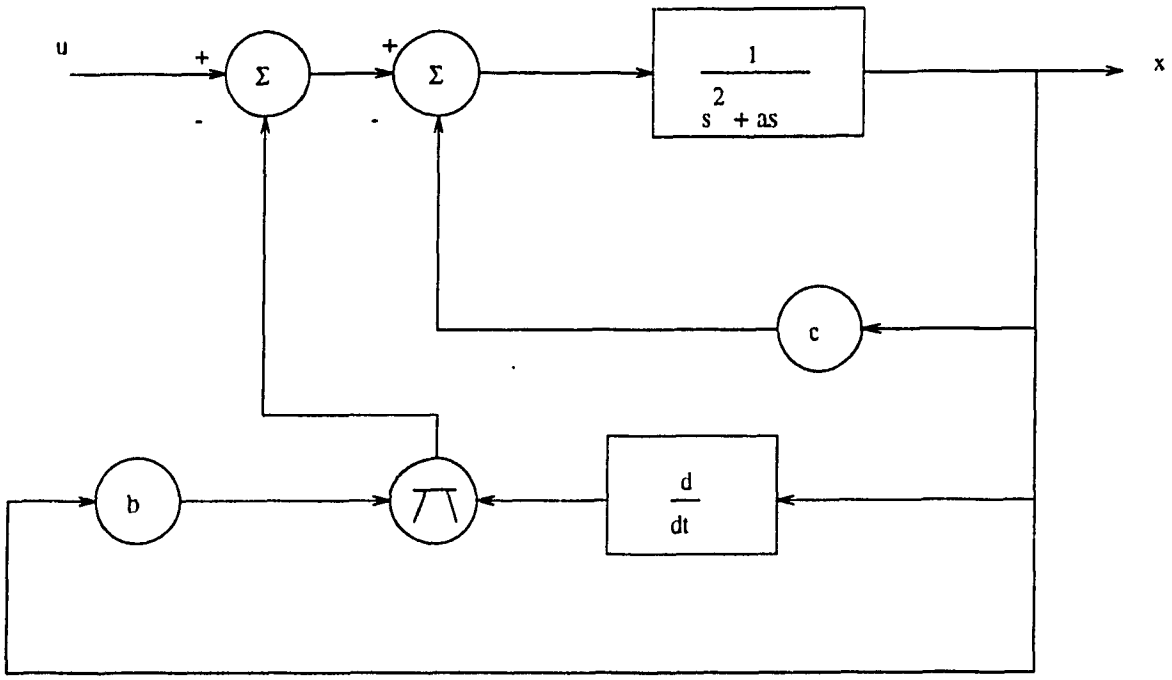

Figure 1.1: A nonlinear feedback system.

Chapter 2

Literature Survey

2.1 Introduction

As explained in the previous chapter, there are some drawbacks to the use of constant-gain controllers for controlling HVAC systems. These can be overcome by using adaptive control. During the last decade, several different schemes for automatic tuning of controllers have been suggested [15], [24]. Several commercial controllers with automatic tuning facilities based on these ideas have also appeared on the market. However, these products have so far been directed toward industrial process control applications. It is only recently that adaptive control has started to appear in building management systems.

This chapter is organized as follows. In section 2.2, the previous work on adaptive control implementation for HVAC systems is given. Difficulties in using these adaptive control methods are identified. In order to overcome these difficulties, it is necessary to design multivariable adaptive controllers for HVAC systems. To this end, the objectives of the thesis are stated in section 2.3.

2.2 Adaptive Control for HVAC Systems: A Survey

In this section a survey of the published literature on the application of adaptive control techniques to HVAC systems is presented. The papers which are surveyed are given in [16]-[27]. In reference [16], Nesler has used self-tuning techniques for controlling a first-order linear thermal process. This process consists of an air handling unit which is used for comfort conditioning. The whole set up consists of 5 blocks: A set of automatic tuning routines to establish initial parameter estimates; a recursive least-squares estimator for estimating process parameters on-line; a control design block which computes the control input; a proportional-integral controller; and a performance monitor which supervises the self-tuning controller operation.

System flexibility and robustness have been increased by the use of the performance monitor. It determines when retuning of the controller is required. The process parameters are estimated on-line using the recursive least-squares (RLS) method described in [30], [31]. Open-loop tests are used for estimating the process gain, the effective deadtime, and the time constant. Proportional and integral control input is derived by minimizing the integrated absolute error for setpoint changes. A forgetting factor is also used to discount the old data and thus track parameter changes.

The main drawback of the control technique mentioned in [16] is that some times self-tuners fail to give proper estimates under certain conditions such as when there are large and unmodeled load disturbances acting on a process. In that event, self-tuning control loop will become unstable. These types of disturbances are common in HVAC processes.

Wallonborg [17] has used pole placement techniques based on input-output models to control a process whose discrete-time transfer function is calculated from wave forms of a periodic oscillation obtained with a relay feedback tuning experiment. An important feature of this technique is the automatic selection of the sampling interval and desired closed-loop poles with respect to the process dynamics. In the tuning experiment, three different discrete-time models are identified. A number of model validation tests are carried out to select the best process model from three possible alternatives. When an appropriate discrete-time model has been selected, the corresponding continuous-time model parameters are used to select a suitable new sampling interval.

In the desired closed-loop system, the denominator polynomial is selected so that two dominant poles are obtained, corresponding to a continuous-time system with a relative damping of 0.7 and a natural frequency, ω. The selection of the desired natural frequency is related to the oscillation frequency obtained from the tuning experiment. The observer poles are at the origin. The control input is calculated by solving the Diophantine equation.

This new algorithm is tested on an HVAC plant in which an air-handling unit is used for heating the outdoor air before it is distributed to the interior of the building. The air is heated in two steps. First, the incoming air is pre-heated by a rotary heat exchanger that recovers excess heat energy from the return air before it leaves the building. Then the supply air is heated to the desired level with a heating coil. In the second experimental application, an auto-tuner is used to control the static pressure in a VAV system. Experimental results reveal the validity of the proposed control scheme.

Its main drawbacks are that in some cases it may be difficult to obtain the

necessary steady-state conditions in a tuning experiment. One such example is the control of hot water supply system where the consumption of water exhibits large fluctuations during normal operation. In many HVAC systems, there is a close interaction between different control loops. Thus, when using an auto-tuner, it is important to select the order in which the loops are tuned so the interaction is minimized.

In reference [18], Pinnella and others have used integral control action with self-tuning capability which critically damps the system response to step inputs. A real-time control algorithm is developed and tested on two different HVAC control systems: (1) static pressure control of a variable air volume fan system, and (2) supply-water temperature control of an experimental steam-to-hot-water converter system. The reason for using integral control action only, as given in [18], is to get good steady-state performance, and only the integral gain has to be adjusted during the tuning process.

The control input is a function of the system gain, time delay, and time constant which are determined from two open-loop experiments. In the first experiment, the system gain is determined, and in the second experiment, the time delay and time constant of the system are determined. The time required for tuning the controller i.e. to conduct the two open-loop experiments is certainly less than the time taken by an operator. After computing the control input by means of open-loop tests, the controller is put into the closed-loop mode and satisfactory results are obtained. The self-tuning procedure produces a gain which provides a nearly critically damped response to a set point change. Results show that the self-tuning controller is effective for systems with slow or fast responses.

The control scheme described in [18] is not fully adaptive. For example, when

the disturbance acting on the system changes then the open-loop experiments have to be repeated for computing the system gain, time delay, and time constant.

Nesler [19] has reported the application of a computer-assisted controller tuning program, an automated tuning controller, and a self-tuning controller to HVAC processes. A process model is estimated for calculating proportional-integral (PI) controller parameters.

An open-loop experiment is done on a mixed-air temperature process to determine the process deadtime, time constant, and process gain. These parameters are then used in computing the tuning constants for PI controllers in model-based controller tuning. Since this tuning method may not provide satisfactory results over a wide range of operation, the author has devised automated controller tuning methods which are summarized in the next few paragraphs.

The first method described is computer-assisted controller tuning. In this method, an operator is assisted by means of a personal computer in tuning DDC controllers by an open-loop step-test method. Pre-processing and numerical analysis of the data by computer are the main factors in reducing the time required to properly tune PI controllers.

The next step in automating controller tuning is to adapt the open-loop step-test method for direct use in the DDC controller. This is called automatic controller tuning. Unlike PC-based methods, the automatic tuning controller requires little operator involvement while tuning. The user specifies a step input size, sampling interval, and high/low alarm values before initiating the tuning routine. Automatic tuning on a regular basis adapts control parameters to changing process conditions. An experiment is performed on a steam-heating coil during set point changes after automatic tuning. Despite a short process time constant, all of the controlled

responses are shown to be within an acceptable region.

A self-tuning controller is also developed after automatic controller tuning. In this, the process model is continuously estimated in real-time using closed-loop control data. Automatic tuning routine is used to establish initial process parameter estimates. Parameters of a PI controller are calculated based on estimated process parameters. A performance monitor is also used to supervise the operation of the self-tuning controller. Testing of the self-tuning controller is performed on an air-handling unit used in comfort conditioning. Experimental results revealed that the self-tuning controller tries to regulate the output variable under different load conditions. The drawback of these techniques is that they cannot be used for nonlinear multi-input, multi-output systems.

Townsend *et al.* [20] have used optimization in terms of appropriate costs and performance functions subject to practical limits using the Pontryagin maximum principle. First the cost function is specified in which different weights are given on the various control inputs, startup conditions, and the deviations of controlled states from their desired steady-state values. The Hamiltonian used in the maximum principle, is maximized using bang-bang control, interior maximization, and singular conditions. It is shown that singular and interior controls cannot be optimal for the given system. Simulation results show the effectiveness of optimal control using bang-bang control theory. Its main drawback is that the controller computations are based on actual process parameters, i.e. it assumes that the process is fully known, which may not be true in a real sense.

In reference [21], Curtiss *et al.* have used neural networks to implement a predictive controller on an HVAC system. The back-propagation learning rule is applied on a neural network to learn the dynamic behavior of the coil model. A

wide range of coil operating data is used to train the network. The proposed scheme involves two neural network controllers: one to perform the actual prediction of the output, and the other to find the correct controller output based upon the error driven by the first network. The results of this method are compared with PID control strategies. It is shown that with a proper choice of the learning rate, the performance of the predictive neural network controller may be better than that of the PID controller. However experimental results show that this technique works fine for simple single order HVAC processes. Several problems can arise when the same neural network is trained using data obtained from a multi-input, multi-output HVAC system.

In [22], a self-tuning start control scheme is developed. The control algorithms are based on a semi-empirically derived relationship between pre-heat time and the measured variables. The behavior of the control scheme is first investigated using a hybrid control simulation of the building and a heating plant. Its performance is evaluated experimentally using a simplified form of the control algorithm which is implemented on a microprocessor-based controller. Results verify the validity of the self-tuning concepts for starting operations of a thermal plant. This scheme is not fully adaptive in the sense that self-tuning is applied only during the start-up operation. The system under consideration is assumed to be completely known which in a real sense is very difficult.

In reference [23], practical considerations are discussed for the implementation of an adaptive controller for a typical HVAC system. In reference [24], PID control parameters are calculated automatically. First the process response to a test signal is sampled and then characteristic values of the process are estimated from the sampled data. By using a performance index, optimal values of the PID control

parameters are calculated. Pole-zero cancellations and root locus techniques are used to control a first-order HVAC process in [25]. In [26], a multi-loop self tuning control scheme to control the air-handling unit is discussed. The use of cascaded loops is proposed to improve the reliability of the self-tuning control. A simplified parameter estimator which incorporates exponential weighting of the past data and a two level forgetting factor is used in [27]. Implementation of this stochastic-approximation-like algorithm is recommended because it is algebraically much simpler than a full recursive least-squares estimator, though, the parameters take longer to converge.

From the above literature review, we note that several adaptive control techniques exist for controlling HVAC systems. However, as pointed out in the review, they also have some limitations. To overcome these limitations, we propose a new control technique which uses servomechanism control strategies along with adaptive gains.

2.3 Objectives of the Thesis

The objectives of the thesis are:

1. To design an adaptive controller for a multivariable, nonlinear MFCH system which will have following properties:

   (a) Regulation against static and dynamic disturbances.

   (b) Continuous adaptation to changing system operating conditions.

   (c) Robustness in the sense that the performance of the controlled dynamic system should be insensitive to changes in its environment and/or its parameters and modeling errors.

   (d) Robust performance to unknown system dynamics. If there are changes in the plant dynamics due to prolonged operation, the controller should adjust itself to compensate for these changes.

2. To prove stability of the closed-loop system.

3. To examine the closed-loop response of the system to realistic changes in operating conditions and external disturbances; also verify the robustness properties and system response to unmodeled dynamics.

In the chapters that follow, we have designed and implemented a controller which satisfies the above mentioned objectives.

Chapter 3

Modeling and Controller Design

3.1 Introduction

In this chapter, physical and analytical models of the MFCH system are given and a controller is designed based on solving the robust servomechanism problem. This chapter is organized as follows: A physical model of the MFCH plant is given in section 3.2. The non-linear dynamic equations describing the physical model are given in section 3.3. From this model, we can see the coupling between different units of the MFCH system. Open-loop simulation results are presented in section 3.4 which show that, in dynamic model, the different components of the MFCH system are properly integrated and respond well to changes in all control inputs. In section 3.5, a robust controller is designed by solving the servomechanism problem. Control techniques used in linear control theory, i.e., pole placement and LQR, are used to obtain the gain matrices. The chapter is summarized in section 3.6

3.2 Physical Model

In northern climates, heating of indoor environmental spaces or zones in buildings is accomplished with several different types of HVAC systems. In this thesis, we consider one specific HVAC system known as a multi-zone fan-coil heating (MFCH) system. Schematic diagram of the MFCH plant is shown in Figure 3.1. The major elements of the system are:

1. Two environmental zones
2. Fan-Coil Units
3. Boiler
4. Ductwork
5. Control Valves
6. Pump
7. Feedback control system.

The operation of the MFCH system can be understood by tracing the path of water around the loop. The boiler heats the water which returns from the individual fan-coil units through the return pipe. The input to the boiler is natural gas which is burnt inside a combustion chamber. The valve C3 controls the rate of flow of natural gas. The rate of flow of hot water to the fan-coil units is regulated via the control valves C1 and C2. A fan is used to circulate air across the fan-coil unit. Thus the air is heated in the coil and delivered to the zones to satisfy the heating load requirements. For thermal comfort, the air leaving the coil must be at an

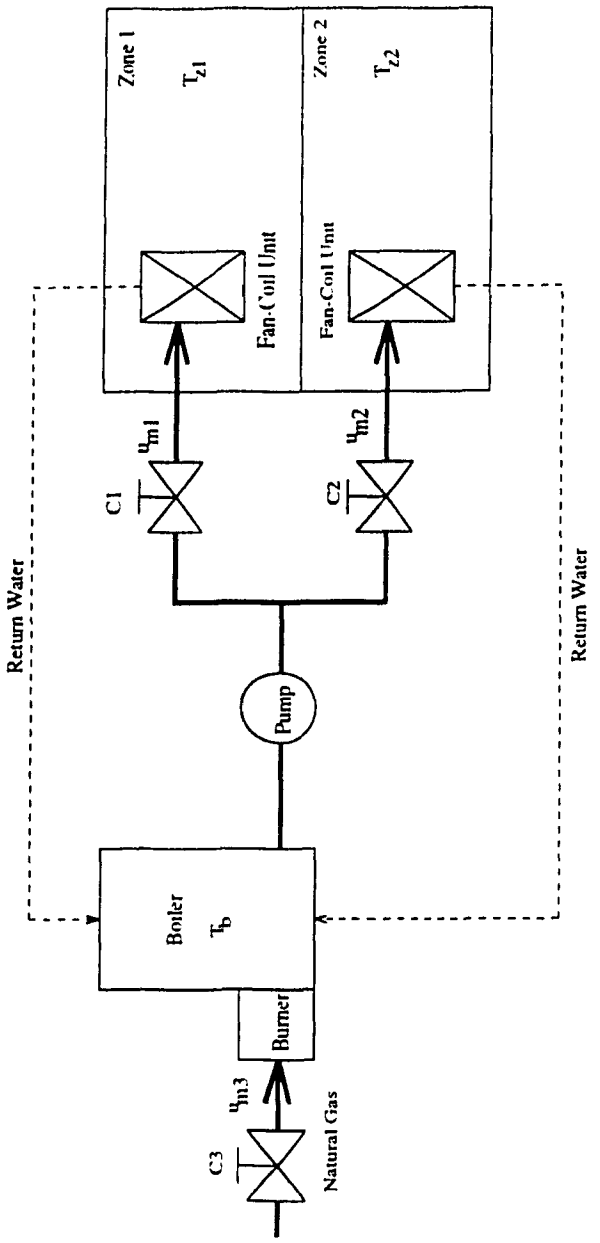

Figure 3.1: Schematic diagram of a multi-zone fan-coil heating (MFCH) system.

appropriate temperature. Furthermore, for good control of zone temperature, the rate of supply water must be continuously modulated.

As shown in the Figure 3.1, there are three control variables u_{m1}, u_{m2}, and u_{m3} which are the mass flow rates of hot water to zones 1 and 2, and the normalized input energy to the boiler respectively. These three control variables are continuously modified to improve the overall response. For example, the mass flow rate of hot water to zones 1 and 2 is controlled by appropriately opening/closing control valves C1 and C2 respectively. The third control input u_{m3} regulates the input energy required to heat the water to the appropriate temperature.

All three control actions require feedback signals from the two zones and the boiler. When the zone temperature decreases because of an increase in heating load, the difference between the set-point and the actual value of the output increases. This output error is fed back via the controllers in order to initiate the control action. Control action includes the modulation of the valves C1 and C2 such that the mass flow rate of the hot water to the fan-coil units is increased, and control of the valve C3 such that the flow rate of natural gas is increased sufficiently to meet the increased heating load. It must be noted that all the control actions are coupled in the sense that the action of one influences the other. Therefore the effects of a changing load on the overall performance of the system must be carefully incorporated into the control strategy.

3.3 Analytical Model

By applying the energy conservation principle and assuming that the zone tempera tures and the boiler temperature remain uniform, the lumped capacity method was

applied to describe the dynamics of the MFCH system (Figure 3.1) by the following nonlinear equations.

$$C_{z1}\frac{dT_{z1}}{dt} = u_{m1}\xi_z(T_b - T_{z1}) - a_{z1}(T_{z1} - T_a) - a_{z12}(T_{z1} - T_{z2}) + hA_{d_1}(T_{d_{11}} - T_{z1}) \quad (3.1)$$

$$C_{z2}\frac{dT_{z2}}{dt} = u_{m2}\xi_z(T_b - T_{z2}) - a_{z2}(T_{z2} - T_a) + a_{z12}(T_{z1} - T_{z2}) + hA_{d_2}(T_{d_{12}} - T_{z2}) \quad (3.2)$$

$$C_b\frac{dT_b}{dt} = u_{m3}(1 - \alpha\frac{T_b}{T_{b_{max}}}) - a_b(T_b - T_p) - u_{m1}\xi_z(T_b - T_{z1}) - u_{m2}\xi_z(T_b - T_{z2}) \quad (3.3)$$

where $u_{m_i} = u_i u_{i_{max}}$, $i = 1, 2, 3$, is the control input through the i^{th} control valve; and u_1, u_2, and u_3 are normalized with respect to their maximum values $u_{1_{max}}$, $u_{2_{max}}$, and $u_{3_{max}}$ respectively. The design parameters of the MFCH system used in this thesis are given in Table 3.1. The physical parameters of the boiler and the zones were chosen by applying the steady-state sizing methods described in [28]. In developing the model equations, we have also assumed that the heat transfer coefficients such as h, ξ_z and the heat loss coefficients a_{z1}, a_{z2}, a_{z12} etc. remain constant. However, in actual systems, these parameters are likely to change. To address this issue, we are interested in designing robust controllers which give good tracking performance even when the system parameters change.

Equations (3.1) and (3.2) describe the energy balance for the respective environmental zones. For example, for zone 1, the rate of energy stored in the air mass of zone 1 is equated to the energy input to the zone via the fan-coil unit, the heat loss to the outdoor environment through the enclosure, heat loss or gain to the adjacent zone, and the interactions in terms of heat loss or gain between the zone air and the thick walls of the enclosure (the last term in equations (3.1) and (3.2)).

Similarly an energy balance on the boiler, equation (3.3), was written by equating the rate of energy stored in the boiler to the energy input from the combustion chamber, heat loss from the exterior surfaces to the boiler room, and heat delivered to the fan-coil units.

The state equations described in equations (3.1)-(3.3) can be written in the following form.

$$\frac{dT_{z1}}{dt} = u_1 C_1(T_b - T_{z1}) - C_2(T_{z1} - T_a) - C_3(T_{z1} - T_{z2}) + f_1(T_{d_{11}} - T_{z1}) \tag{3.4}$$

$$\frac{dT_{z2}}{dt} = u_2 C_4(T_b - T_{z2}) - C_5(T_{z2} - T_a) + C_6(T_{z1} - T_{z2}) + f_2(T_{d_{12}} - T_{z2}) \tag{3.5}$$

$$\frac{dT_b}{dt} = u_3 C_7(1 - \alpha\frac{T_b}{T_{b_{max}}}) - C_8(T_b - T_p) - u_1 C_9(T_b - T_{z1}) - u_2 C_{10}(T_b - T_{z2}) \tag{3.6}$$

where

$$C_1 = u_{1_{max}}\xi_z/C_{z1}$$

$$C_2 = a_{z1}/C_{z1}$$

$$C_3 = a_{z12}/C_{z1}$$

$$C_4 = u_{2_{max}}\xi_z/C_{z2}$$

$$C_5 = a_{z2}/C_{z2}$$

$$C_6 = a_{z12}/C_{z2}$$

$$C_7 = u_{3_{max}}/C_b$$

$$C_8 = a_b/C_b$$

$$C_9 = u_{1_{max}}\xi_z/C_b$$

$$C_{10} = u_{2_{max}}\xi_z/C_b$$

$$f_1 = hA_{d_1}/C_{z1}$$

$$f_2 = hA_{d_2}/C_{z2}$$

Most building enclosure elements (such as walls, floor etc.) store energy and release it to the indoor environment. In other words, they introduce thermal lag effects. It has been shown in a previous study [29] that this behavior of the walls can be described by a fifth-order linear model. We have adopted this model, in this thesis so that the environmental zones can be represented by equations (3.1) and (3.2), together with a fifth-order dynamic disturbance model representing the storage fluxes released by the enclosure walls. The solar gains entering the zones strike the interior surfaces of the enclosure walls. This is modeled by the term $Q_{d_1}w$ and $Q_{d_2}w$ in equations (3.7) and (3.8). This process is dynamic in nature. In other words, the solar gains striking the interior surfaces are absorbed by the walls and later released to the indoor air in zones 1 and 2. Thus, these storage fluxes released by the walls act as slow, time varying disturbances on zone 1 and 2. It is for this reason they are referred to as dynamic disturbances in this thesis. The dynamic disturbance models for zones 1 and 2 are given by

$$\begin{aligned} \dot{\mathbf{T}}_{\mathbf{d_1}} &= P_{d_1}\mathbf{T}_{\mathbf{d_1}} + Q_{d_1}w + R_{d_1}T_{z1} \\ T_{d_{11}} &= S_{d_1}\mathbf{T}_{\mathbf{d_1}} \end{aligned} \tag{3.7}$$

$$\begin{aligned} \dot{\mathbf{T}}_{\mathbf{d_2}} &= P_{d_2}\mathbf{T}_{\mathbf{d_2}} + Q_{d_2}w + R_{d_2}T_{z2} \\ T_{d_{12}} &= S_{d_2}\mathbf{T}_{\mathbf{d_2}} \end{aligned} \tag{3.8}$$

where

$$P_{d_1} = \begin{bmatrix} -5.724 & 5.112 & 0.6228 & 0 & 0 \\ 1.43 & -2.86 & 1.43 & 0 & 0 \\ 0 & 1.43 & -2.86 & 1.43 & 0 \\ 0 & 0 & 1.43 & -2.86 & 1.43 \\ 0 & 0 & 0 & 5.112 & -5.112 \end{bmatrix}, \; Q_{d_1} = \begin{bmatrix} 5.8845 \\ 0 \\ 0 \\ 0 \\ 0 \end{bmatrix},$$

$$R_{d_1} = \begin{bmatrix} 0.6228 \\ 0 \\ 0 \\ 0 \\ 0 \end{bmatrix}, \; S_{d_1} = \begin{bmatrix} 1 & 0 & 0 & 0 & 0 \end{bmatrix},$$

$$P_{d_2} = P_{d_1}, \; Q_{d_2} = Qd_1, \; R_{d_2} = R_{d_1}, \; S_{d_2} = S_{d_1}$$

As we can see from the dynamic equations (3.4), (3.5), and (3.6), the normalized control inputs are u_1, u_2, and u_3. Thus the system outputs of interest such as the temperature of zone 1 (T_{z1}), the temperature of zone 2 (T_{z2}), and the temperature of the boiler (T_b), are maintained at their desired set-points by controlling one or all of the following control inputs.

1. Normalized mass flow rate of water through control valve C1, i.e. u_1.

2. Normalized mass flow rate of water through control valve C2, i.e. u_2.

3. Normalized mass flow rate of natural gas through control valve C3, i.e. u_3.

The important question is how to determine the feedback control algorithms for u_1, u_2, and u_3. But before we go further in designing control strategies, it is instructive to look at the open-loop characteristics of the MFCH system. The open-loop

responses will provide the adequacy of the overall MFCH system and also give an indication of the time required by the states to reach their steady values.

3.4 Open-Loop Simulation Results

Figure 3.2 shows the open-loop response of the MFCH system. The control inputs u_1, u_2, and u_3 are held constant at 0.5, 0.4, and 0.4 respectively and the outdoor temperature was assumed to remain constant at $-10.0\,\text{deg}\,C$. Under this constant inputs and disturbances the zone temperature T_{z1}, after starting from an initial temperature of $20\,\text{deg}\,C$, increases exponentially and reaches a steady-state value of $23.26\,\text{deg}\,C$ in about 40,000 minutes (650 hours). Similarly T_{z2} and T_b also increase exponentially from initial conditions of $20\,\text{deg}\,C$ and $70\,\text{deg}\,C$ and reach steady-state values of $21.27\,\text{deg}\,C$ and $57.98\,\text{deg}\,C$ respectively in about same time, i.e. 40,000 minutes.

If there are step changes in the control inputs, say, $u_1 = 0.6$, $u_2 = 0.5$, and $u_3 = 0.5$, even then the MFCH system output reaches steady state as shown in Figure 3.3. Since we have increased the control inputs, the steady-state values of T_{z1}, T_{z2}, and T_b are higher than the steady-state values shown in the Figure 3.2.

Thus the results shown in the Figures 3.2 and 3.3 give an indication that the component models are properly integrated and the responses from the integrated model are satisfactory. However, the important thing to note at this point is that the MFCH system responds to changes in the control inputs u_1, u_2, and u_3.

Also shown in Figure 3.4 are the open-loop responses of the system when the initial conditions are perturbed by $1.0\,\text{deg}\,C$ from their operating point (steady-state values in Figure 3.2) while the states describing the dynamic disturbances were

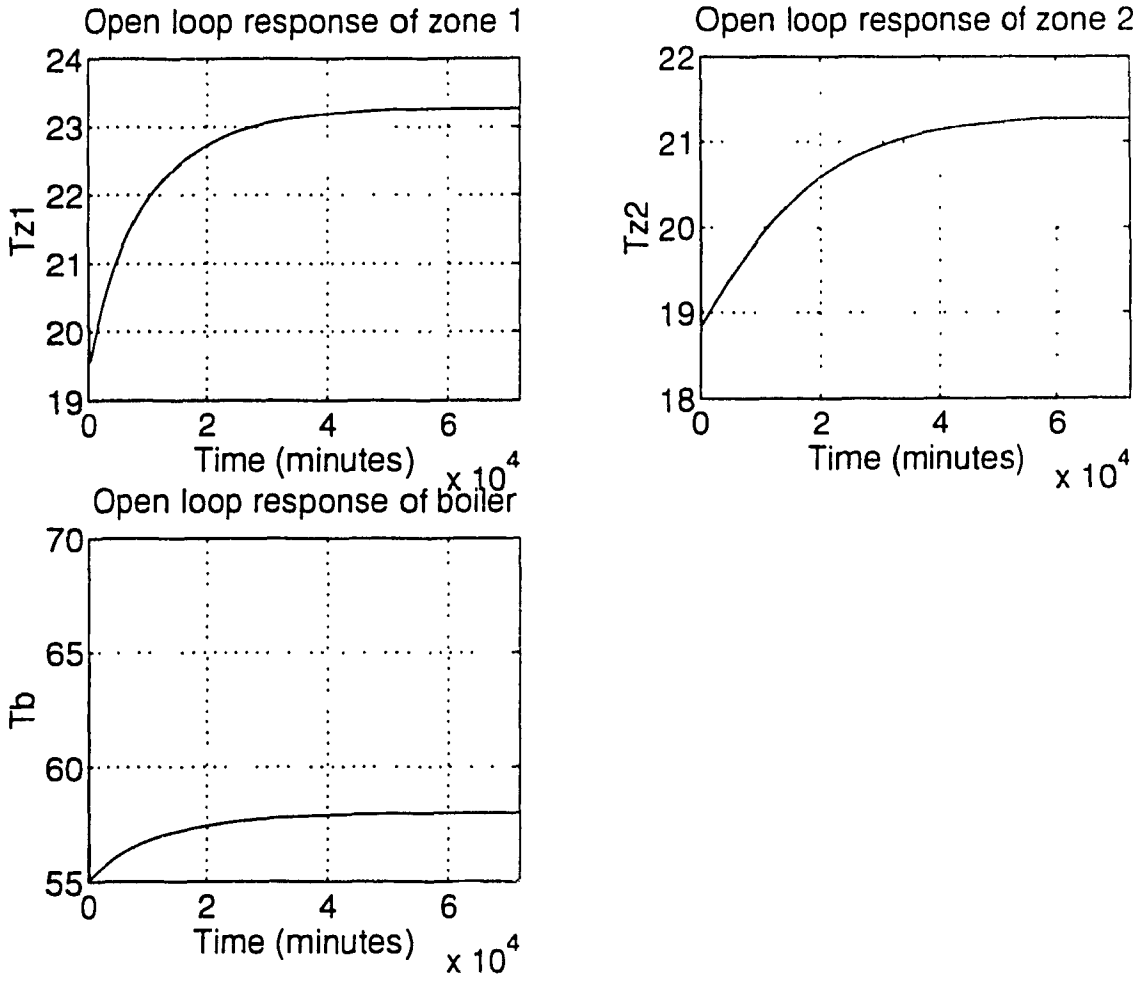

Figure 3.2: Open-loop response of the MFCH system.

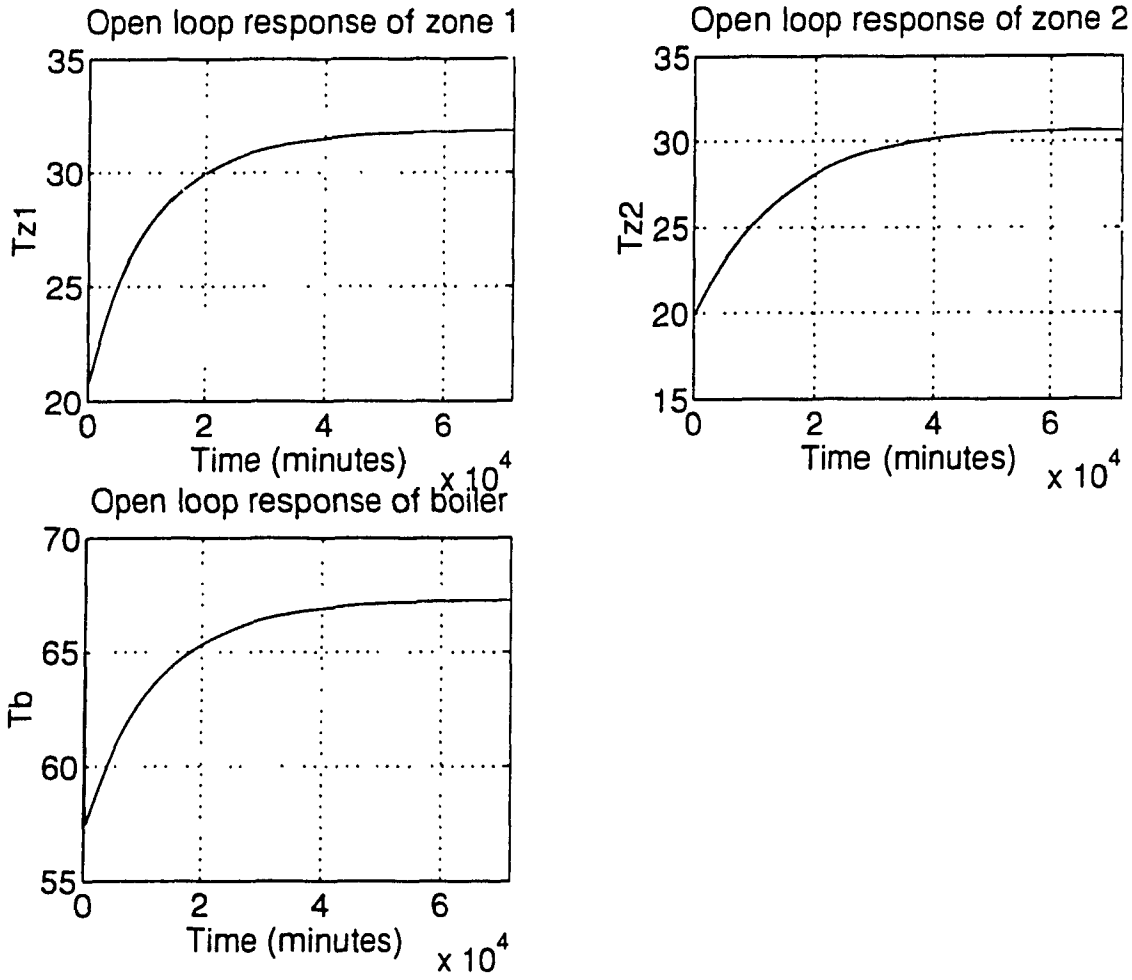

Figure 3.3: Effect of step changes in the control input on the open-loop response of the MFCH system.

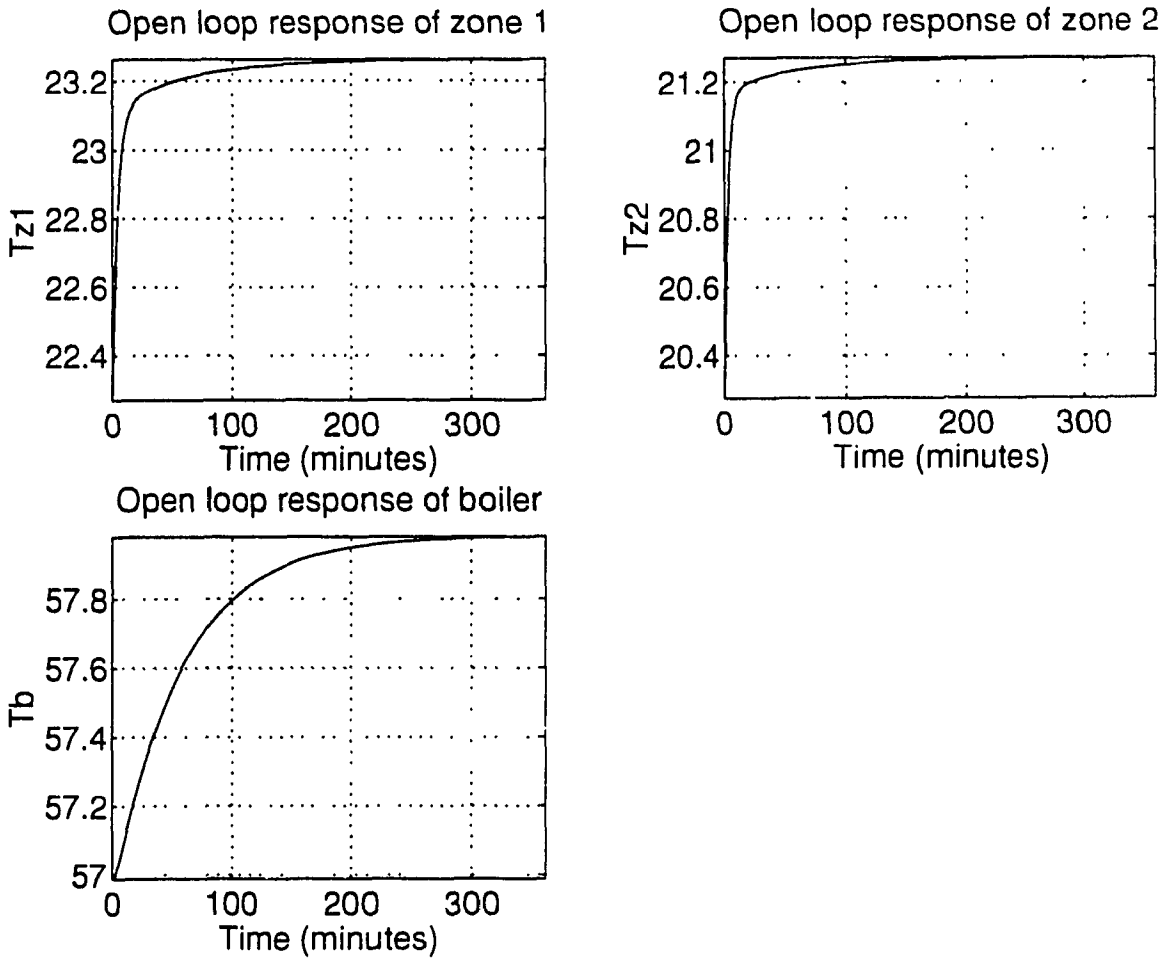

Figure 3.4: Open-loop response of the system when the initial conditions are perturbed by 1.0 deg C.

held at the operating values. The system's response in this case is fast. The zone temperatures T_{z1}, T_{z2} take about three hours and the boiler temperature T_b takes about 5 hours to reach steady state. In other words, when the initial conditions of the dynamic disturbance model are far away from the steady-state values (for the results shown in Figure 3.2 the initial conditions of states describing the dynamic disturbance model were $\mathbf{T_{d_1}}(0) = 20\deg C$, $\mathbf{T_{d_2}}(0) = 20\deg C$ which are about $-4.0\deg C$ away from their respective steady state values) the system takes longer time to reach steady state.

Now the main task is to develop an algorithm for controlling u_1, u_2, and u_3 such that T_{z1}, T_{z2}, and T_b are maintained at the desired set-points. Thus we are interested in seeking methods by which the control inputs u_1, u_2, and u_3 are automatically adjusted through feedback control.

3.5 Controller Design

In this section, a robust controller has been developed based on solving the robust servomechanism problem for the MFCH system given by equations (3.4) -

The desired performance of the closed-loop system includes asymptotic tracking/regulation in the presence of input disturbances and arbitrary perturbations in the plant parameters of the system. The MFCH plant is assumed to be unknown. The continuous-time least square (CTLS) algorithm is used to estimate the linear model of the nonlinear MFCH system at each operating point. The estimated parameters are used in the design of the controller. The controller consists of three parts: 1) a servocompensator, 2) a stabilizing compensator, and 3) an estimation-error compensator. The servocompensator is a feedback compensator with error

inputs and consists of a number of unstable subsystems (equal to the number of the outputs to be regulated) with identical dynamics which depend on the disturbances and reference inputs to the system. Servocompensator corresponds to the generalization of the integral controller of classical control theory. The stabilizing compensator stabilizes the resultant system obtained by applying the servocompensator to the plant. The sole purpose of the estimation-error compensator is to provide compensation for the estimation error resulting from the use of a linear estimator to obtain a model for the nonlinear MFCH system at each operating point.

The nonlinear equations (3.4)-(3.6) can be written in the following form:

$$\dot{\mathbf{x}} = \mathcal{F}_n(\mathbf{x}(t), \mathbf{u}(t), \mathbf{d_s}(t), \mathbf{d_d}(t)) \tag{3.9}$$

where $\mathbf{x} \in \Re^n$, $\mathbf{u} \in \Re^m$, $\mathbf{d_s} \in \Re^{l_s}$, and $\mathbf{d_d} \in \Re^{l_d}$ are the state vector, the control input vector, the static disturbance vector, and the dynamic disturbance vector of lengths n, m, l_s, and l_d respectively.

We have developed control strategies for the MFCH system defined by equation (3.9) using LQR and pole placement theory. To this end, we first assume that the nonlinear system described by equation (3.9) is piecewise linear and its linear model about some operating point $(\mathbf{x_o}, \mathbf{u_o}, \mathbf{d_{s_o}}, \mathbf{d_{d_o}})$ is given by

$$\Delta\dot{\mathbf{x}} = A\Delta\mathbf{x}(t) + B\Delta\mathbf{u}(t) + F_s\Delta\mathbf{d_s}(t) + F_d\Delta\mathbf{d_d}(t) \tag{3.10}$$

where $\Delta\mathbf{x}(t)$, $\Delta\mathbf{u}(t)$, $\Delta\mathbf{d_s}(t)$, and $\Delta\mathbf{d_d}$ are deviations from the operating point values of the state vector, the control input vector, the static disturbance vector, and the dynamic disturbance vector. The matrices F_s and F_d can be put in one matrix as $F = [F_s \vdots F_d]$. Equation (3.10) can then be written as

$$\Delta\dot{\mathbf{x}} = A\Delta\mathbf{x}(t) + B\Delta\mathbf{u}(t) + F\Delta\mathbf{d}(t) \tag{3.11}$$

where

$$\Delta \mathbf{d}(t) = \begin{bmatrix} \Delta \mathbf{d_s}(t) \\ \Delta \mathbf{d_d}(t) \end{bmatrix}$$

The linear system described by equation (3.11) is obtained by linearizing the nonlinear system (3.9) using a Taylor series expansion. Equation (3.11) is a linear approximation of the nonlinear system (3.9) about some operating point, and is likely to change from its nominal value during continuous operation of the plant. Therefore, it can be concluded that the system (3.11) may not exactly represent the nonlinear system at different operating points. Thus, while designing a controller for such a system, the designer should take into account the effect of perturbations in the linear model. In other words, the resulting controller should be robust.

3.5.1 Problem Statement

The linear model of the MFCH system about an operating point is described by the following equations.

$$\begin{aligned} \Delta \dot{\mathbf{x}}(t) &= A\Delta \mathbf{x}(t) + B\Delta \mathbf{u}(t) + F\Delta \mathbf{d}(t) \\ \Delta \mathbf{y}(t) &= \Delta \mathbf{x}(t) \\ \mathbf{e}(t) &= \Delta \mathbf{y}(t) - \Delta \mathbf{y_r}(t) \end{aligned} \tag{3.12}$$

where $\Delta \mathbf{y}(t) \in \Re^p$ is the output vector of the linear model, $\Delta \mathbf{y_r}(t) \in \Re^p$ is the reference vector and $\mathbf{e}(t) \in \Re^p$ is the vector of the tracking error.

The servocompensator is used in series with the actual system. The servocompensator contains the dynamics of the reference signal $\Delta \mathbf{y_r}(t)$ and the disturbance vector $\Delta \mathbf{d}(t)$ [32], [33]. This aspect of the design is called the *internal model principle*. The servocompensator's main function is to make the error $\mathbf{e}(t)$ asymptotically

approach zero. It is assumed that the disturbance vector $\Delta\mathbf{d}(t)$ satisfies the following equations.

$$\Delta\mathbf{d}(t) = C_d\Delta\mathbf{z_d}(t) \tag{3.13}$$

$$\Delta\dot{\mathbf{z}}_\mathbf{d}(t) = A_d\Delta\mathbf{z_d}(t) \tag{3.14}$$

where $\Delta\mathbf{z_d}(t) \in \Re^{n_d}$. The pair (C_d, A_d) is observable. The initial conditions $\Delta\mathbf{z_d}(t_0)$ may be known or unknown. For a step disturbance, i.e. $s = 0$, equations (3.13) and (3.14) can be written as:

$$\Delta\mathbf{d}(t) = \Delta\mathbf{z_d}(t) \tag{3.15}$$

$$\Delta\dot{\mathbf{z}}_\mathbf{d}(t) = 0 \tag{3.16}$$

where $A_d = 0$, $C_d = 1$, and $\Delta\mathbf{z_d}(t_0) = M_d$. M_d is the magnitude of the step disturbance.

For a sinusoidal disturbance, i.e. $s^2 + w_d^2 = 0$, equations (3.13) and (3.14) can be written as:

$$\Delta\mathbf{d}(t) = \begin{bmatrix} 1 & 0 \end{bmatrix}\Delta\mathbf{z_d}(t) \tag{3.17}$$

$$\Delta\dot{\mathbf{z}}_\mathbf{d}(t) = \begin{bmatrix} 0 & 1 \\ -w_d^2 & 0 \end{bmatrix}\Delta\mathbf{z_d}(t) \tag{3.18}$$

where $A_d = \begin{bmatrix} 0 & 1 \\ -w_d^2 & 0 \end{bmatrix}$, $C_d = \begin{bmatrix} w_d & 0 \end{bmatrix}$, and $\Delta\mathbf{z_d}(t_0) = \begin{bmatrix} 0 \\ M_d \end{bmatrix}$. M_d is the amplitude of the sinusoidal disturbance.

The reference signal vector $\Delta\mathbf{y_r}(t)$ satisfies the following equations:

$$\Delta\mathbf{y_r}(t) = C_r\Delta\mathbf{z_r}(t) \tag{3.19}$$

$$\Delta\dot{\mathbf{z}}_\mathbf{r}(t) = A_r\Delta\mathbf{z_r}(t) \tag{3.20}$$

where $\Delta \mathbf{z_r}(t) \in \Re^{n_r}$. The pair (C_r, A_r) is observable. $\Delta \mathbf{z_r}(t_0)$ is the known initial condition. We assume that all the outputs are available for measurements. For a step reference signal, i.e. $s = 0$, equations (3.19) and (3.20) can be written as:

$$\Delta \mathbf{y_r}(t) = \Delta \mathbf{z_r}(t) \tag{3.21}$$

$$\Delta \dot{\mathbf{z}}_\mathbf{r}(t) = 0 \tag{3.22}$$

where $A_r = 0$, $C_r = 1$, and $\Delta \mathbf{z_r}(t_0) = M_r$. M_r is the magnitude of the step reference signal.

For a sinusoidal reference signal, i.e. $s^2 + w_r^2 = 0$, equations (3.19) and (3.20) can be written as:

$$\Delta \mathbf{y_r}(t) = \begin{bmatrix} 1 & 0 \end{bmatrix} \Delta \mathbf{z_r}(t) \tag{3.23}$$

$$\Delta \dot{\mathbf{z}}_\mathbf{r}(t) = \begin{bmatrix} 0 & 1 \\ -w_r^2 & 0 \end{bmatrix} \Delta \mathbf{z_r}(t) \tag{3.24}$$

where $A_r = \begin{bmatrix} 0 & 1 \\ -w_r^2 & 0 \end{bmatrix}$, $C_r = \begin{bmatrix} w_r & 0 \end{bmatrix}$, and $\Delta \mathbf{z_r}(t_0) = \begin{bmatrix} 0 \\ M_r \end{bmatrix}$. M_r is the amplitude of the sinusoidal reference signal.

As it is already stated, servocompensator consisting of the nature of the *outside world* is used in series with the actual system. The constraint that the overall augmented system be stable might require the use of the stabilizing compensator. The stabilizing compensator will be designed using linear control theory in next section.

Now the control problem can be defined as follows: Construct a controller for the nonlinear system (3.9) using adaptive gains for the stabilizing controller derived from linear control theory (pole placement and LQR) and using the available

measurements $\mathbf{x}(t)$ such that the resulting closed-loop system is stable, and the error $\mathbf{e}(t) \rightarrow 0$ as $t \rightarrow \infty$ for all $\mathbf{x}(t_0) \in \Re^n$ and for all disturbances and reference inputs satisfying (3.13), (3.14), (3.19), and (3.20).

3.5.2 Controller Structure

Let $q_d(s)$ and $q_r(s)$ be the minimal polynomials of A_d and A_r respectively. Let $q(s) = s^r + q_1 s^{r-1} + \cdots + q_r$ be the monic least common multiple of $q_d(s)$ and $q_r(s)$.

The necessary and sufficient conditions for solving the robust servomechanism problem are summarized as follows [32], [33].

1. (A, B) is a stabilizing pair,

2. (C, A) is a detectable pair,

3. The number of inputs is greater than or equal to the number of outputs, i.e. $m \geq p$, and

4. $\text{rank}\begin{bmatrix} A - \lambda_i I & B \\ C & D \end{bmatrix} = n + p, \quad i = 1, 2, 3, ..., r$

When conditions 1-4 are satisfied then a robust controller can be constructed. As shown in the Figure 3.5, such a controller consists of two parts (i) a servocompensator, and (ii) a stabilizing compensator. The servocompensator's main function is to cancel the effect in the steady-state of the disturbances acting on the system, and to provide asymptotic tracking. The stabilizing compensator provides overall stability of the closed-loop system and improves the system's transient behavior. As stated earlier, we are interested in designing a robust controller for the nonlinear system, while assuming that the model parameters are unknown. By using the

Variable Name	Description	Numerical Value
T_{z1}	Temperature of zone 1	-
T_{z2}	Temperature of zone 2	-
T_b	Temperature of boiler	-
C_{z1}	Thermal capacity of air in zone 1	374 $KJ/\deg C$
C_{z2}	Thermal capacity of air in zone 2	250 $KJ/\deg C$
C_b	Boiler thermal capacity	836 $KJ/\deg C$
a_{z1}	Heat loss coefficient of zone 1	740 $KJ/(h-\deg C)$
a_{z2}	Heat loss coefficient of zone 2	540 $KJ/(h-\deg C)$
a_b	Heat loss coefficient of boiler surfaces	54 $KJ/(h-\deg C)$
a_{z12}	Inter zone heat loss coefficient	27 $KJ/(h-\deg C)$
ξ_z	Heat transfer coefficient	0.6 $KJ/(Kg-\deg C)$
α	Boiler fuel loss parameter	0.12
$u_{1_{max}}$	Max. mass flow rate of water through valve 1	1850 (Kg/h)
$u_{2_{max}}$	Max. mass flow rate of water through valve 2	1350 (Kg/h)
$u_{3_{max}}$	Max. capacity of burner	90000 (Kj/h)
T_p	Boiler room temperature	20.0 $\deg C$
T_a	Outdoor temperature	-10.0 $\deg C$
$T_{b_{max}}$	Max. temperature of the boiler	90.0 $\deg C$

Table 3.1: List of symbols with their nominal values.

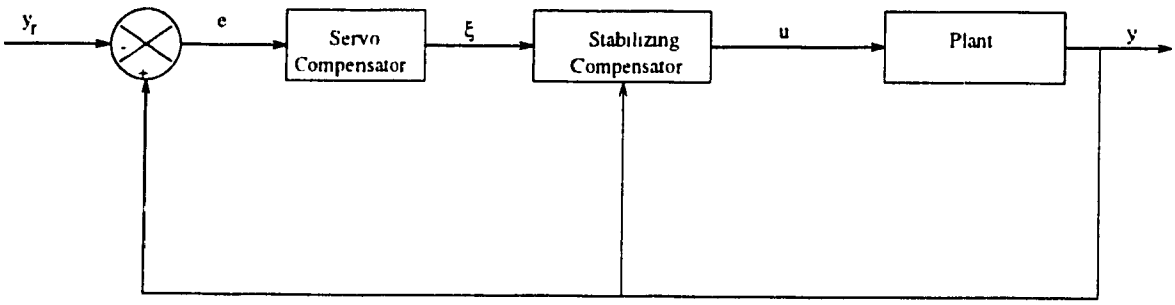

Figure 3.5: A robust controller for the servomechanism problem

continuous-time least squares (CTLS) algorithm [39], [40], we estimate the matrices A and B of the linear system (3.11) at each instant of time, and then use the estimated A and B for the design of the robust controller. The estimates of A and B are represented by $\hat{A}$ and $\hat{B}$ respectively. The estimated model is given by

$$\Delta\dot{\hat{\mathbf{x}}} = \begin{bmatrix} \hat{A} & \hat{B} \end{bmatrix} \begin{bmatrix} \Delta\mathbf{x}(t) \\ \Delta\mathbf{u}(t) \end{bmatrix} \tag{3.25}$$

where $\begin{bmatrix} \Delta\mathbf{x}(t) \\ \Delta\mathbf{u}(t) \end{bmatrix} \in \Re^{n+m}$ is the input vector to the estimator. The estimation error is given as

$$\mathbf{e}_s(t) = \Delta\dot{\mathbf{x}}(t) - \Delta\dot{\hat{\mathbf{x}}}(t) \tag{3.26}$$

Or in other words,

$$\Delta\dot{\mathbf{x}}(t) = \Delta\dot{\hat{\mathbf{x}}}(t) + \mathbf{e}_s(t) \tag{3.27}$$

Linear models of the nonlinear system (3.9) are estimated at each instant of the time by the CTLS algorithm, and $\Delta\mathbf{x}$ and $\Delta\mathbf{u}$ are used in the estimator. The control law is then given by

$$\Delta\mathbf{u} = -K_1\Delta\xi - K_2\Delta\mathbf{x} - K_3\mathbf{e}_s \tag{3.28}$$

where $\Delta\xi \in \Re^{pr}$ is the output of servocompensator [41], [33] defined by:

$$\Delta\dot{\xi}(t) = \Omega^*\Delta\xi(t) + \theta^*\mathbf{e}(t) \tag{3.29}$$

$$\Omega^*(t) = \tau \ \text{blockdiag}(\Omega, \Omega, \cdots, \Omega)_{\text{p times}}\tau^{-1} \tag{3.30}$$

$$\theta^*(t) = \tau\theta \tag{3.31}$$

where τ is a non-singular real matrix and θ is chosen so that (Ω^*, θ^*) is a controllable

pair; $\Omega(r \times r)$ is a matrix in companion form, and is computed as follows:

$$\Omega(t) = \begin{bmatrix} 0 & 1 & 0 & \cdots & 0 \\ 0 & 0 & 1 & \cdots & 0 \\ \vdots & \vdots & \vdots & \vdots & \vdots \\ -q_r & -q_{r-1} & -q_{r-2} & \cdots & -q_r \end{bmatrix}$$

By combining equations (3.25), (3.27) and (3.29), the open-loop augmented system can be formed as:

$$\begin{bmatrix} \Delta\dot{\mathbf{x}} \\ \Delta\dot{\xi} \end{bmatrix} = \begin{bmatrix} \hat{A} & 0 \\ 0 & \Omega^* \end{bmatrix} \begin{bmatrix} \Delta\mathbf{x} \\ \Delta\xi \end{bmatrix} + \begin{bmatrix} \hat{B} \\ 0 \end{bmatrix} \Delta\mathbf{u} + \begin{bmatrix} I \\ 0 \end{bmatrix} \mathbf{e}_s + \begin{bmatrix} 0 \\ \theta^* \end{bmatrix} \mathbf{e} \quad (3.32)$$

Since the desired reference vector, $\Delta\mathbf{y}_r$, is zero, output error in equation (3.32) can be written as:

$$\mathbf{e} = \Delta\mathbf{y} - \Delta\mathbf{y}_r \quad (3.33)$$

$$= \Delta\mathbf{y} \quad (3.34)$$

$$= \Delta\mathbf{x} \quad (3.35)$$

Hence equation (3.32) can written as:

$$\begin{bmatrix} \Delta\dot{\mathbf{x}} \\ \Delta\dot{\xi} \end{bmatrix} = \begin{bmatrix} \hat{A} & 0 \\ \theta^* & \Omega^* \end{bmatrix} \begin{bmatrix} \Delta\mathbf{x} \\ \Delta\xi \end{bmatrix} + \begin{bmatrix} \hat{B} \\ 0 \end{bmatrix} \Delta\mathbf{u} + \begin{bmatrix} I \\ 0 \end{bmatrix} \mathbf{e}_s \quad (3.36)$$

Since the pair (Ω^*, θ^*) is controllable, it is clear that the pair $\left(\begin{bmatrix} \hat{A} & 0 \\ \theta^* & \Omega^* \end{bmatrix}, \begin{bmatrix} \hat{B} \\ 0 \end{bmatrix} \right)$ is stabilizable. Hence stabilizing compensator can be designed or in other words matrices K_1 and K_2 can be designed using linear control theory such that the augmented system described by (3.36) is stable.

By substituting for $\Delta\mathbf{u}$ from equation (3.28) into (3.36), we obtain the following closed-loop system:

$$\begin{bmatrix} \Delta\dot{\mathbf{x}} \\ \Delta\dot{\xi} \end{bmatrix} = \begin{bmatrix} \hat{A} - \hat{B}K_2 & -\hat{B}K_1 \\ \theta^* & \Omega^* \end{bmatrix} \begin{bmatrix} \Delta\mathbf{x} \\ \Delta\xi \end{bmatrix} + \begin{bmatrix} I - \hat{B}K_3 \\ 0 \end{bmatrix} \mathbf{e}_s \tag{3.37}$$

The matrices K_1 and K_2 are obtained by solving the LQR or pole placement problem and K_3 is computed using Lyapunov theory such that the overall closed-loop system given by (3.37) is stable. The pole placement and LQR design are given in the following sections. The computation of K_3 and the proof of stability of the closed-loop system are given in Chapter 4.

3.5.3 Pole Placement Problem

Since all the states of the augmented open-loop system (3.36) are available for measurement, the pole placement technique has been used to move the poles of the open-loop system (3.36) to a specified set of locations in the s-plane.

The control law given in equation (3.28) can be written as

$$\begin{aligned} \Delta\mathbf{u}(t) &= -K_1\Delta\xi(t) - K_2\Delta\mathbf{x}(t) - K_3\mathbf{e}_s(t) \\ &= -\begin{bmatrix} K_2 & K_1 \end{bmatrix} \begin{bmatrix} \Delta\mathbf{x}(t) \\ \Delta\xi(t) \end{bmatrix} - K_3\mathbf{e}_s(t) \qquad (3.38) \\ &= -K\Delta\mathbf{z}(t) - K_3\mathbf{e}_s(t) \qquad (3.39) \\ &= \Delta\mathbf{u}_{sm}(t) + \Delta\mathbf{u}_{es}(t) \qquad (3.40) \end{aligned}$$

where $K = \begin{bmatrix} K_2 & K_1 \end{bmatrix}$; $\Delta\mathbf{z}(t) = \begin{bmatrix} \Delta\mathbf{x}(t) \\ \Delta\xi(t) \end{bmatrix}$; $\Delta\mathbf{u}_{sm}(t) = -K\Delta\mathbf{z}(t)$; and $\Delta\mathbf{u}_{es}(t) = -K_3\mathbf{e}_s(t)$

The open-loop augmented system given by equation (3.36) can be written as

$$\Delta\dot{\mathbf{z}}(t) = \Lambda\Delta\mathbf{z}(t) + \Theta\Delta\mathbf{u}(t) + \Theta_I\mathbf{e}_s(t) \tag{3.41}$$

where $\Lambda = \begin{bmatrix} \hat{A} & 0 \\ 0^* & \Omega^* \end{bmatrix}$; $\Theta = \begin{bmatrix} \hat{B} \\ 0 \end{bmatrix}$; and $\Theta_I = \begin{bmatrix} I \\ 0 \end{bmatrix}$

By substituting (3.39) in (3.41), we get the following closed-loop system:

$$\Delta\dot{\mathbf{z}}(t) = \left[\Lambda - \Theta K \right] \Delta\mathbf{z}(t) + \left[\Theta_I - \Theta K_3 \right] \mathbf{e}_s(t) \tag{3.42}$$

Now we determine the gain matrix K such that the $\left[\Lambda - \Theta K \right]$ has a desired set of eigenvalues λ_i; $i = 1, 2, \cdots (pr + n)$. This problem has been investigated by several researchers and many algorithms already exist for solving the problem by state feedback [34],[36],[37],[38]. Conventional technique [38] of solving pole placement problem require a reduction of a system to a canonical form. The coefficients of the characteristic polynomial of the open-loop and desired closed-loop systems are compared to obtain the feedback vector. This approach is numerically unreliable because the roots of the polynomial are sensitive to perturbations in its coefficients and ill-conditioning is associated with the reduction of the system to its canonical form. An accurate and efficient approach to solve the pole placement problem is developed by Patel and Misra [34]. This algorithm can be regarded as the inverse of the implicitly QR algorithm for eigenvector determination. More details concerning this algorithm are given in [35].

3.5.4 LQR Problem

The equation (3.41) can be written as

$$\Delta\dot{\mathbf{z}}(t) = \Lambda\Delta\mathbf{z}(t) + \Theta\Delta\mathbf{u}_{\mathbf{sm}}(t) + \Theta\Delta\mathbf{u}_{\mathbf{es}}(t) + \Theta_I\mathbf{e}_s(t) \tag{3.43}$$

The gain matrix K for this system can be designed by minimizing a quadratic cost function of the state $\Delta\mathbf{z}(t)$ and the control input $\Delta\mathbf{u}_{\mathbf{sm}}(t)$. The quadratic cost function is defined as

$$J = \int_0^t (\Delta \mathbf{z}^{\mathbf{T}}(\mathbf{t}) Q \Delta \mathbf{z}(t) + \Delta \mathbf{u}_{\mathbf{sm}}^{\mathbf{T}}(t) R \Delta \mathbf{u}_{\mathbf{sm}}(t)) dt \tag{3.44}$$

where the matrices Q and R denote the weighting on system's state $\Delta \mathbf{z}(\mathbf{t})$ and the control input $\Delta \mathbf{u}_{\mathbf{sm}}(\mathbf{t})$ respectively; and Q is a positive semi-definite matrix and R is a positive definite matrix. These matrices are chosen according to the relative importance of the cost of control and the cost of deviations from the desired state. The solution to equation (3.44) is given in [33.45] as

$$\Delta \mathbf{u}_{\mathbf{sm}}(t) = -R^{-1}\Theta^T P \Delta \mathbf{z}(t) \tag{3.45}$$

$$= K \Delta \mathbf{z}(t) \tag{3.46}$$

where $K = -R^{-1}\Theta^T P$, and P is a $(pr + n) \times (pr + n)$ symmetric matrix which is the unique positive semi-definite solution of the algebraic Riccati equation

$$\Lambda^T P + P\Lambda - P\Theta R^{-1}\Theta^T P + Q = 0 \tag{3.47}$$

The gain matrix, K i.e. matrices K_1 and K_2, are determined at each operating point. We have used both pole placement and LQR design for this purpose. The open-loop augmented system (3.36) is also updated at each instant of time.

3.6 Summary

Physical and analytical models of the MFCH system have been described. Open-loop tests were made to check the proper integration of different components. A controller has been designed by assuming the system's dynamics as completely unknown. A linear model estimator has been used to identify the linear model of the nonlinear system at each operating point. Pole placement and LQR control design methods

have been proposed for computing the gain matrices K_1 and K_2 at each operating point.

Chapter 4

Stability and Implementation

4.1 Introduction

In the previous chapter, a quantitative analysis of the MFCH dynamical system has been done by formulating a set of mathematical equations that describe its behavior. Even though the open-loop system is stable, the performance of the resulting closed-loop system (with the designed controller) may not be satisfactory [42]. The implication is that the closed-loop system should not only give good performance but also be stable. The concept of stability has been investigated extensively in the literature [47], [48]. The stability theory of Lyapunov [49], and input-output stability theory based on functional analysis techniques, are the two general approaches that are used most widely. Here we use the direct method of Lyapunov to give a mathematical proof of stability of the closed-loop system.

This chapter is organized as follows. In section 4.2, an analytical proof of the stability of the closed-loop system is given. Implementation of the controller is discussed in section 4.3. A short summary of the chapter is given in section 4.4.

4.2 Stability

4.2.1 Lyapunov's Stability Criterion

The general state equation for a nonlinear system can be expressed as

$$\dot{X} = f(X(t), U(t), t) \tag{4.1}$$

An analytical solution of equation (4.1) is in general difficult to obtain. If a numerical solution is tried then the question of stability cannot be fully answered as solutions to an infinite set of initial conditions are needed. Therefore, a number of methods have been devised which yield information about stability without resorting to its complete solution. Lyapunov's direct method is one such method.

Lyapunov's direct method is based on the concept of energy and the relation of stored energy with system stability. Consider an autonomous physical system described by

$$\dot{x} = f(x(t)) \tag{4.2}$$

and let $x(x(t_0), t)$ be a solution corresponding to an initial condition $x(t_0)$. Further, let $V(x)$ be the total energy associated with the system. If the derivative $\dot{V}(x)$ is negative for all $x(x(t_0), t)$ except at its equilibrium points, then it follows that the energy of the system decreases as t increases and finally the system will reach an equilibrium point. This holds because energy is a non-negative function of the system states. The energy reaches a minimum only when the system reaches steady-state. These ideas are used to derive a mathematical proof of stability for the MFCH system.

Equation (3.37) can be written as:

$$\Delta\dot{\mathbf{z}}(t) = \Phi\Delta\mathbf{z}(t) + \mu_1\mathbf{e}_s(t) \tag{4.3}$$

where

$$\Delta \mathbf{z}(t) = \begin{bmatrix} \Delta \mathbf{x} \\ \Delta \xi \end{bmatrix}, \quad \Phi = \begin{bmatrix} \hat{A} - \hat{B}K_2 & -\hat{B}K_1 \\ \theta^* & \Omega^* \end{bmatrix}, \text{ and } \mu_1 = \begin{bmatrix} I - \hat{B}K_1 \\ 0 \end{bmatrix} \quad (4.4)$$

Since (Ω^*, θ^*) is a controllable pair and K_1 and K_2 are chosen with LQR or pole placement theory we can conclude that matrix Φ is asymptotically stable. A lyapunov function candidate V is chosen as

$$V(\mathbf{z}) = \Delta \mathbf{z}^T P \Delta \mathbf{z} \quad (4.5)$$

where the matrix P is symmetric and positive definite. For stability of system (4.3), we have to ensure that $\dot{V} \leq 0$. It follows from equation (4.5) that

$$\dot{V} = \Delta \dot{\mathbf{z}}^T P \Delta \mathbf{z} + \Delta \mathbf{z}^T P \Delta \dot{\mathbf{z}} \quad (4.6)$$

By substituting equation (4.3) in (4.6), we get the following.

$$\begin{aligned} \dot{V} &= (\Phi \Delta \mathbf{z} + \mu_1 \mathbf{e}_s)^T P \Delta \mathbf{z} + \Delta \mathbf{z}^T P (\Phi \Delta \mathbf{z} + \mu_1 \mathbf{e}_s) \\ &= \Delta \mathbf{z}^T \Phi^T P \Delta \mathbf{z} + \mathbf{e}_s{}^T \mu_1^T P \Delta \mathbf{z} + \Delta \mathbf{z}^T P \Phi \Delta \mathbf{z} + \Delta \mathbf{z}^T P \mu_1 \mathbf{e}_s \\ &= \Delta \mathbf{z}^T (\Phi^T P + P \Phi) \Delta \mathbf{z} + 2 \Delta \mathbf{z}^T P \mu_1 \mathbf{e}_s \end{aligned} \quad (4.7)$$

Since Φ is an asymptotically stable matrix, so for any positive definite matrix Q, there exists a positive definite matrix P which satisfies the following Lyapunov equation.

$$\Phi^T P + P \Phi = -Q \quad (4.8)$$

Since for stability $\dot{V}$ should be less then or equal to zero, by substituting (4.8) in (4.7), we require

$$\dot{V} = -\Delta \mathbf{z}^T Q \Delta \mathbf{z} + 2 \Delta \mathbf{z}^T P \mu_1 \mathbf{e}_s \leq 0 \quad (4.9)$$

Since $-\Delta \mathbf{z}^T Q \Delta \mathbf{z} \leq 0$, for stability, it is sufficient that

$$2\Delta \mathbf{z}^T P \mu_1 \mathbf{e}_s \leq 0$$

$$\text{i.e.} \quad \Delta \mathbf{z}^T P \mu_1 \mathbf{e}_s \leq 0$$

$$\text{i.e.} \quad \Delta \mathbf{z}^T P \begin{bmatrix} I - \hat{B} K_3 \\ 0 \end{bmatrix} \mathbf{e}_s \leq 0$$

which will be satisfied if

$$K_3 = \hat{B}^{-1} \tag{4.10}$$

Since $\mathbf{e}_s$ is bounded (because of the estimation mechanism), it follows that the closed-loop system remains stable if K_3 is chosen as in equation 4.10 and K_1, K_2 are chosen by either pole placement or LQR theory.

4.3 Implementation

Before we describe the details of the robust controller implementation, first we compute the linear model of the MFCH system at the following operating point: $\mathbf{x}_0 = [23.26\ 21.27\ 57.98]^T$, $\mathbf{u}_0 = [0.5\ 0.4\ 0.4]^T$, $T_a = -10.0$, $Td_{11_o} = 24.81$, and $Td_{12_o} = 22.68$. The linear model was obtained by a Taylor's series expansion about this operating point. The matrices A_o, B_o, F_{s_o}, and F_{d_o} of linear model (3.10) are

$$A_o = \begin{bmatrix} 12.89 & 0.07 & 1.48 \\ 0.10 & -17.56 & 1.29 \\ 0.66 & 0.38 & -1.17 \end{bmatrix}, \quad B_o = \begin{bmatrix} 103.0 & 0 & 0 \\ 0 & 118.9 & 0 \\ -46.09 & -35.57 & 99.33 \end{bmatrix}.$$

$$F_{s_o} = \begin{bmatrix} 1.97 \\ 2.16 \\ 0 \end{bmatrix}, \quad F_{d_o} = \begin{bmatrix} 9.35 & 0 \\ 0 & 11.0 \\ 0 & 0 \end{bmatrix}$$

It should be noted here that the linear model given above is used only for the initial guess of the matrices A and B required for the estimator. In the simulation, an initial guess of the matrices A and B was also taken 60-80 % away from the values shown above.

The servocompensator given by equation (3.29) is rewritten as

$$\begin{aligned} \dot{\Delta\xi}(t) &= \Omega^* \Delta\xi(t) + \theta^* \mathbf{e}(t) \\ &= \Omega^* \Delta\xi(t) + \theta^* \Delta\mathbf{x}(t) \end{aligned} \tag{4.11}$$

Since $\Delta\mathbf{y_r}(t) = \Delta\mathbf{x_r}(t) \in \Re^n$ is a zero vector as explained in the previous chapter. From equation (3.20) we have $A_r = 0$ and $C_r = \begin{bmatrix} 1 \\ 1 \\ 1 \end{bmatrix}$

For each output $q_r = s$. Also each state is acted upon by a constant step disturbance i.e. $s = 0$, and a dynamic disturbance, i.e. $s + \alpha = 0$. Thus from equation 3.14, A_d and C_d can be written as

$$A_d = \begin{bmatrix} 0 & 1 \\ 0 & -\alpha \end{bmatrix}, \quad C_d = \begin{bmatrix} 1 & 0 \\ 0 & 1 \end{bmatrix}$$

with unkown $z_d(t_0)$.

Therefore, for each output, $q_d(s) = s(s + \alpha)$. Since $q(s)$ is the monic least common multiple polynomial of $q_r(s)$ and $q_d(s)$, it can be written as

$$q(s) = s(s + \alpha) \tag{4.12}$$

Thus the companion matrix Ω can be written as

$$\Omega = \begin{bmatrix} 0 & 1 \\ 0 & -\alpha \end{bmatrix}$$

Let θ = block diag$(\phi, \phi \cdots, \phi)_{p \text{ times}}$ where $\phi = [0 \ \ 1]^T$.

$$\theta = \begin{bmatrix} 0 & 0 & 0 \\ 1 & 0 & 0 \\ 0 & 0 & 0 \\ 0 & 1 & 0 \\ 0 & 0 & 0 \\ 0 & 0 & 1 \end{bmatrix}$$

If τ is chosen as identity matrix, i.e. $I_{6\times6}$, we can get Ω^* and θ^* as

$$\Omega^* = \begin{bmatrix} 0 & 1 & 0 & 0 & 0 & 0 \\ 0 & -\alpha & 0 & 0 & 0 & 0 \\ 0 & 0 & 0 & 1 & 0 & 0 \\ 0 & 0 & 0 & -\alpha & 0 & 0 \\ 0 & 0 & 0 & 0 & 0 & 1 \\ 0 & 0 & 0 & 0 & 0 & -\alpha \end{bmatrix} \tag{4.13}$$

$$\theta^* = \begin{bmatrix} 0 & 0 & 0 \\ 1 & 0 & 0 \\ 0 & 0 & 0 \\ 0 & 1 & 0 \\ 0 & 0 & 0 \\ 0 & 0 & 1 \end{bmatrix}$$

In equation (4.13), α is the most dominant pole of the dynamic disturbance model given by (3.7) and (3.8). This model is assumed to be unknown. Hence, we estimate α by applying the CTLS algorithm [39], [40] to obtain a first order approximation of (3.7) or (3.8) (since dynamics of (3.7) and (3.8) are the same) using the CTLS algorithm [39], [40].

The augmented matrix shown in equation (3.36) can be written as

$$\begin{bmatrix} \Delta\dot{\mathbf{x}} \\ \Delta\dot{\xi} \end{bmatrix} = \begin{bmatrix} \hat{A}_{3\times3} & \vdots & 0_{3\times6} \\ \theta^{*}_{6\times3} & \vdots & \Omega^{*}_{6\times6} \end{bmatrix} \begin{bmatrix} \Delta\mathbf{x} \\ \Delta\xi \end{bmatrix} + \begin{bmatrix} \hat{B}_{3\times3} \\ 0_{6\times3} \end{bmatrix} \Delta\mathbf{u} + \begin{bmatrix} I_{3\times3} \\ 0_{6\times3} \end{bmatrix} \Delta\mathbf{e}_s \qquad (4.14)$$

The matrices K_1, K_2 are chosen first using pole placement theory, and then using LQR design, and as explained in the previous section K_3 is chosen as $\hat{B}^{-1}$. The gain matrices K_1, K_2, and K_3 are computed at each instant of time, based on the present values of the estimates $\hat{A}$, and $\hat{B}$.

The schematic diagram in Figure 4.1 shows the closed-loop operation of the plant. From the diagram, it is clear that the gain matrices K_1, K_2, and K_3 are updated at each instant of time. The error vector $\mathbf{e}(t)$ goes asymptotically to zero as t approaches infinity.

For the MFCH system, $n = 3$, $m = 3$, $l_s = 1$, $l_d = 2$, $p = 3$, $n_d = 2$, $n_r = 1$, and $r = 2$, the variables used in the model with their dimensions are given in Table 4.1.

4.4 Summary

Lyapunov's direct method has been used to provide the proof of stability of the closed-loop system. With a proper choice of the gain matrix K_3 along with the

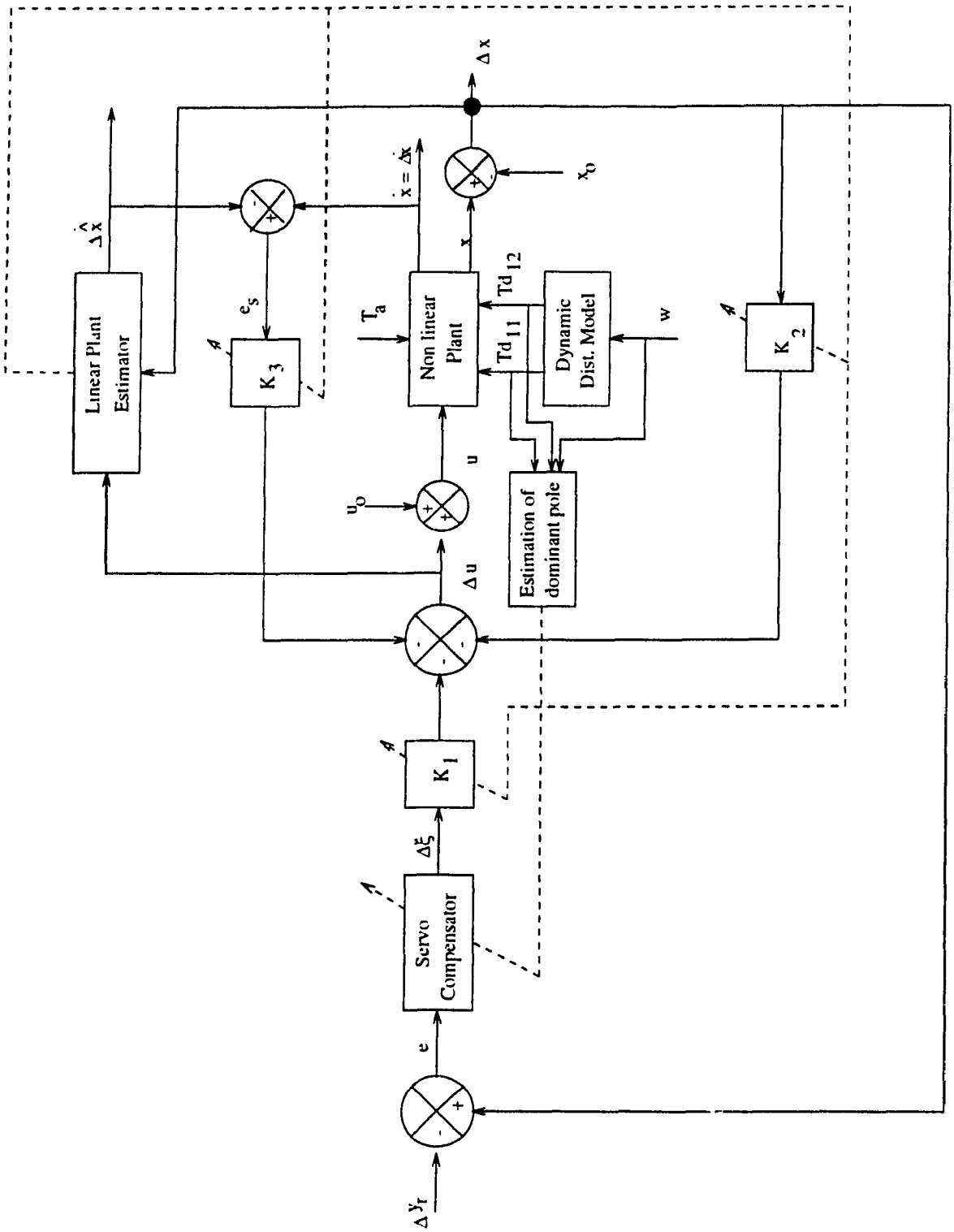

Figure 4.1: Overall configuration of the robust controller for the servomechanism problem

gain matrices K_1 and K_2 obtained using pole placement or LQR design, it has been shown that closed-loop asymptotic stability and tracking can be achieved. The implementation of the closed-loop scheme for the MFCH system has also been discussed.

Symbolic Representation of the variable	Size
$\mathbf{x}$, $\mathbf{u}$	3×1 each
$\mathbf{d_s}$	1×1
$\mathbf{d_d}$	2×1
F_s, F_d	3×1, 3×2 respectively
A, $\hat{A}$	3×3 each
B, $\hat{B}$	3×3 each
F	3×3
$\mathbf{z_d}$, $\mathbf{z_r}$	2×1, 1×1 respectively
A_d, A_r	2×2, 1×1 respectively
$\Delta\mathbf{y_r}$	3×1
$\mathbf{e_s}$	3×1
Ω^*, θ^*	6×6, 6×3 respectively
$\mathbf{e}$, $\Delta\xi$	3×1, 6×1 respectively
K_1, K_2, K_3	3×6, 3×3, 3×3 respectively
ϕ, μ_1,	9×9, 9×3 respectively

Table 4.1: List of symbolic representation of the variables and their sizes

Chapter 5

Results and Discussion

5.1 Introduction

In this chapter, the results of the closed-loop system after controller implementation are presented and discussed. The performance of the system has been studied under realistic operating conditions. This chapter is organized as follows: Section 5.2 contains the effects of step changes in the states of the system, the outdoor temperature, and the dynamic disturbance, on the closed-loop performance of the system when the controller is designed using pole placement and LQR techniques. In section 5.3, the effect of variations in the system parameters such as heat-loss coefficients, effectiveness of the fan-coil units, on the closed-loop system's performance are discussed, and it is shown that the designed controller is robust. The effect of introducting estimation-error feedback is given in section 5.4. In section 5.5, effects of adding some nonlinear dynamics such as valve dynamics on the system's behavior are given. It is shown that the system is insensitive to unmodeled dynamics. In section 5.6, the adaptive controller is tested for new setpoints, and the comparison is made with

fixed-gain controller.

5.2 Effects of Step Changes in Initial Conditions and Disturbances

In this section, the performance of the controller is examined under different operating conditions. In the following simulated test cases, the effects of

1. changing the initial conditions of the system from the operating point,
2. a step change in outdoor temperature (static disturbance), and
3. a step change in the dynamic disturbance due to thermal lag effects of the building (described by the two dynamic disturbance models),

are studied.

The zone temperatures are affected by changes in initial conditions and external disturbances such as outdoor temperature (static disturbance) and solar radiation fluxes striking the inside surfaces of the enclosure walls (dynamic disturbances). These changes can occur concurrently or in several combinations. To simulate these cases, we first consider the following scenario.

Case 1: Initial conditions: perturbed; no static or dynamic disturbances

We consider a cold-day in winter in Montreal with an outdoor temperature equal to $-10.0\,\mathrm{deg}\,C$ (operating point). We also assume that it is an overcast day and therefore the effect of solar gain is negligible. In other words, the solar gain in the dynamic disturbance model is set to zero. Under these conditions, we assume that

due to opening of the door (people entering or leaving the zone) cold-air enters the zone and consequently the zone temperature decreases by $-0.5\,\mathrm{deg}\,C$ from its operating conditions. Furthermore, we have also assumed that the boiler temperature is $-0.5\,\mathrm{deg}\,C$ away from its operating value. Thus initial conditions of the zone temperatures and the boiler temperature are $X_0 = [22.76\ 20.77\ 57.18]^T$. How the controller restores the zone temperature back to their desired setpoints is depicted in Figure 5.1 and Figure 5.2. The results shown were obtained with the designed controller using the pole placement technique (Figure 5.1) and the LQR method (Figure 5.2).

The results shown in Figure 5.1 correspond to the following pole locations which were chosen arbitrarily: -13.0, -9.0, -10.5, -12.0, -13.5, -11.4, -12.6, -11.0, -9.6. As we see from Figure 5.1, all the outputs reach their respective reference values in about 40 minutes. The control inputs also reach their operating point values in about 20 minutes. The overshoot in zone temperatures is within acceptable limits, i.e. it is within 10 % of the reference values.

The Q and R matrices chosen for the LQR method were as:

$$Q = \begin{bmatrix} W_x & 0 & 0 & 0 & 0 & 0 & 0 & 0 & 0 \\ 0 & W_x & 0 & 0 & 0 & 0 & 0 & 0 & 0 \\ 0 & 0 & W_x & 0 & 0 & 0 & 0 & 0 & 0 \\ 0 & 0 & 0 & W_\xi & 0 & 0 & 0 & 0 & 0 \\ 0 & 0 & 0 & 0 & W_\xi & 0 & 0 & 0 & 0 \\ 0 & 0 & 0 & 0 & 0 & W_\xi & 0 & 0 & 0 \\ 0 & 0 & 0 & 0 & 0 & 0 & W_\xi & 0 & 0 \\ 0 & 0 & 0 & 0 & 0 & 0 & 0 & W_\xi & 0 \\ 0 & 0 & 0 & 0 & 0 & 0 & 0 & 0 & 2 \times W_\xi \end{bmatrix} \tag{5.1}$$

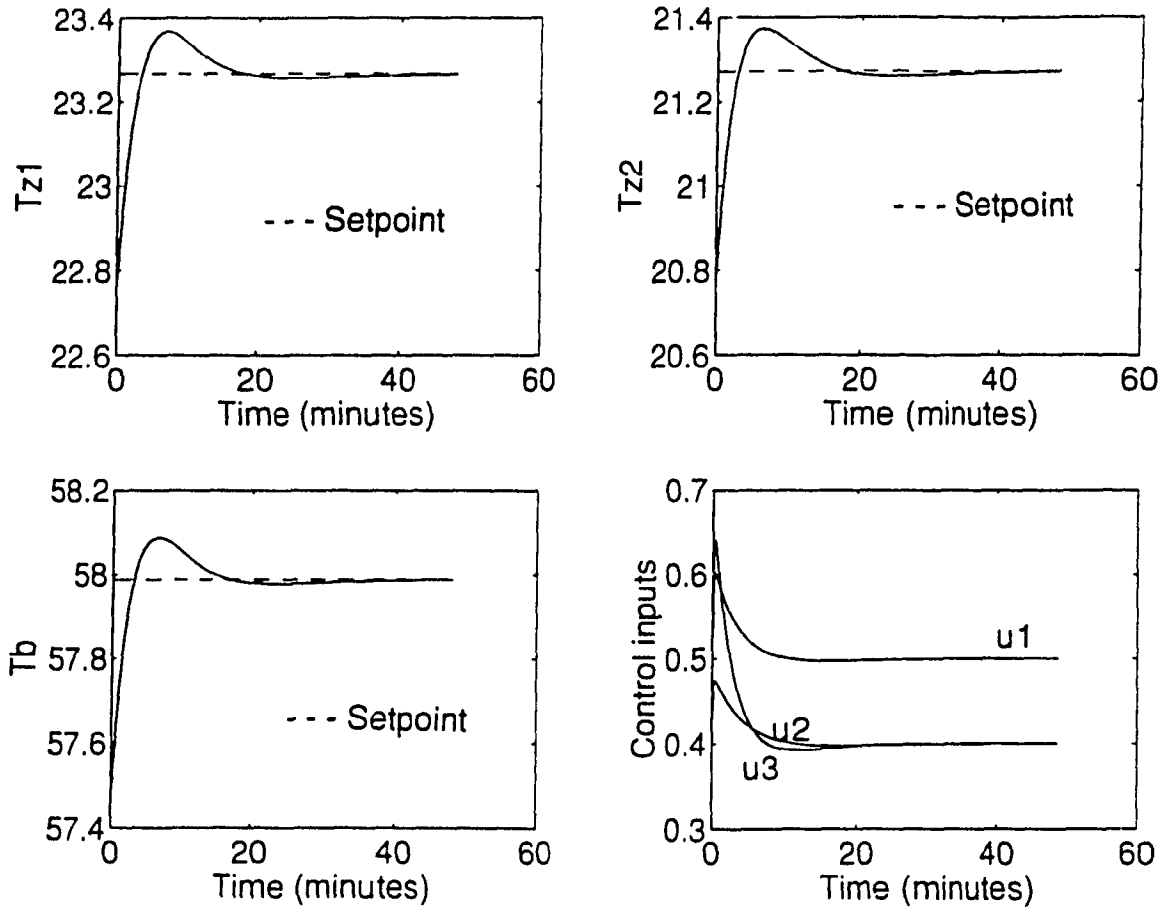

Figure 5.1: Closed-loop response showing the effect of perturbations in the initial conditions for the controller designed using pole placement theory

$$R = \begin{bmatrix} 21.75 & 0 & 0 \\ 0 & 11.25 & 0 \\ 0 & 0 & 5075 \end{bmatrix} \tag{5.2}$$

where $W_x = 0.005$ and $W_\xi = 1.25 \times 10^4$. As shown in Figure 5.2, the response of the system is quite fast as compared to the pole placement design, and all the outputs reach their corresponding setpoints in about 7 minutes.

In all the simulations that follow, when the controller is designed using the LQR method, the matrices Q and R given in equation (5.1) and (5.2), are used.

Case 2: Initial conditions: perturbed; static disturbance; no dynamic disturbances

In this simulation, we consider a $-5.0\,\mathrm{deg}\,C$ step change in outdoor air temperature (static disturbance), while all other conditions remain the same as those used in the previous case. The outdoor response of the system to the above changes are depicted in Figures 5.3 (pole placement design) and 5.4 (LQR design). As we see in Figure 5.3, all the outputs go to their corresponding reference values in about 40 minutes and in 7 minutes in Figure 5.4. Note that at steady state, the magnitudes of the control inputs are higher than their nominal values. This increase in the control inputs is the energy required to offset the effect of a $-5.0\,\mathrm{deg}\,C$ change in the outdoor temperature. It may be noted that the system responses in Figure 5.4 are faster than those in Figure 5.3.

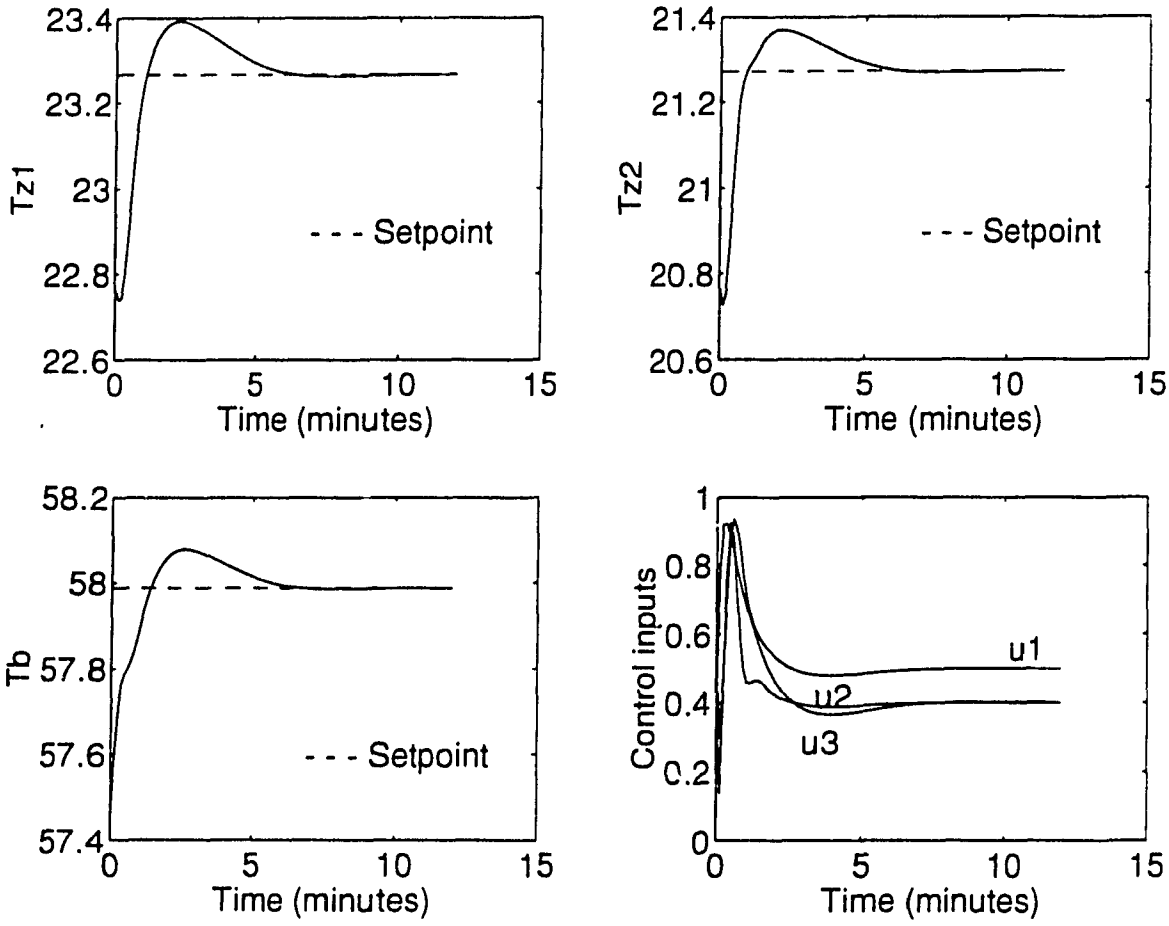

Figure 5.2: Closed-loop response showing the effect of perturbations in the initial conditions for the controller designed using LQR theory.

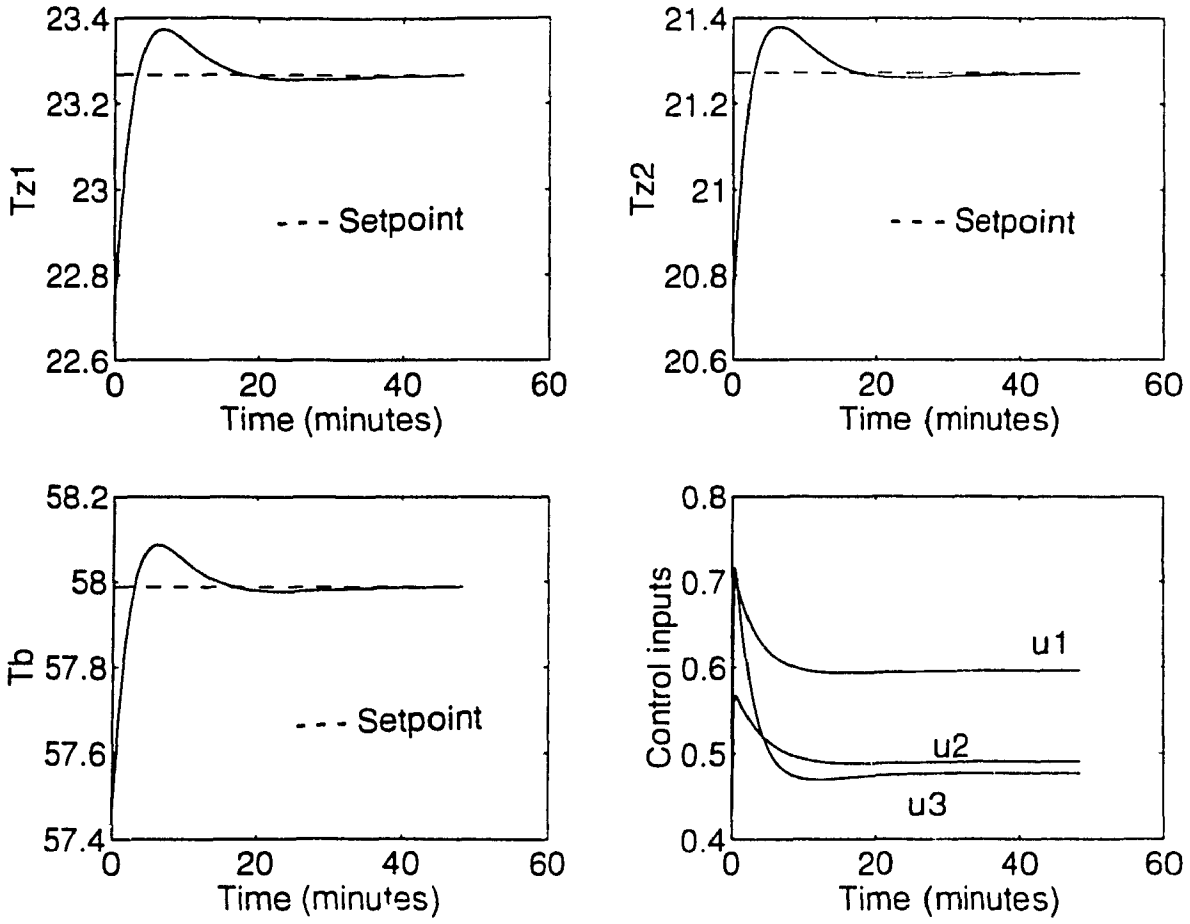

Figure 5.3: Closed-loop response showing the effect of perturbations in initial conditions and static disturbance for the controller designed using pole placement theory

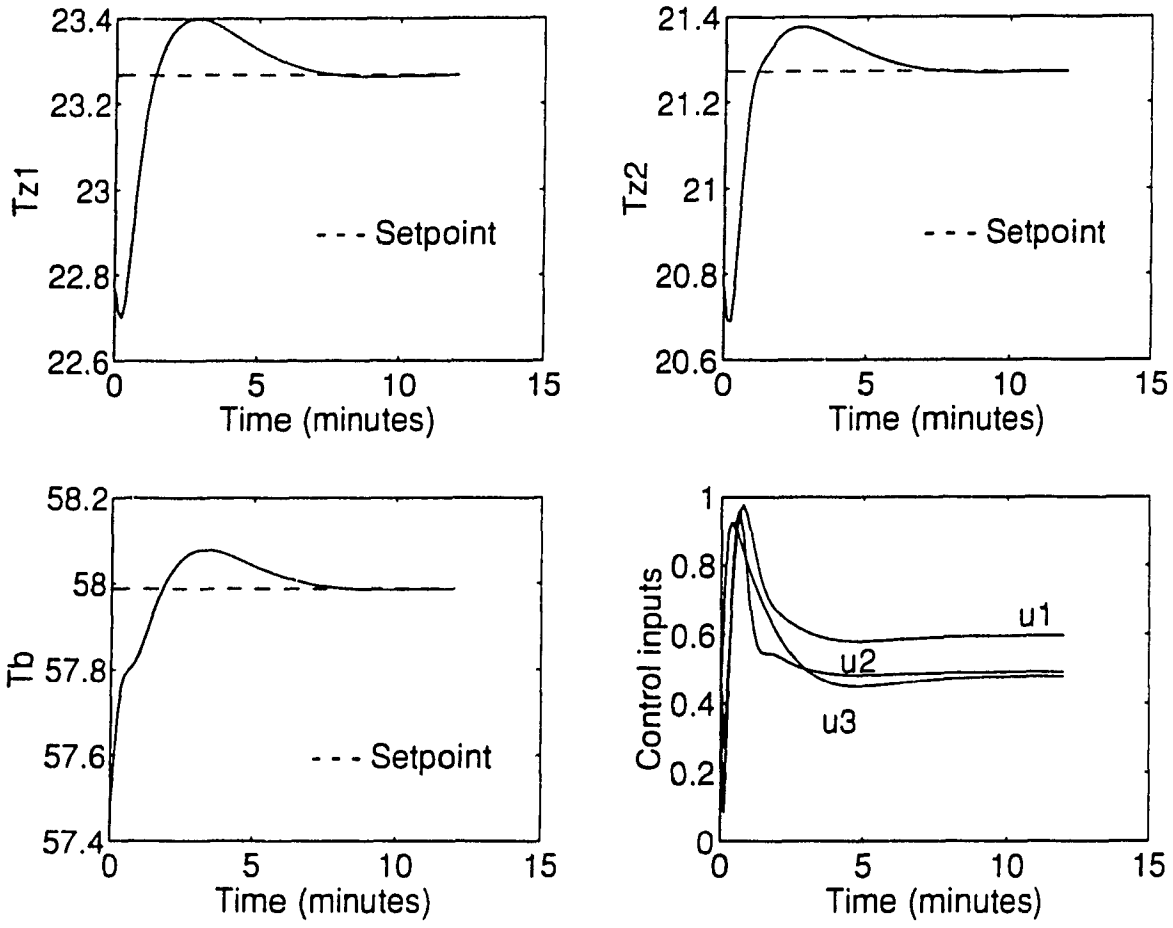

Figure 5.4: Closed-loop response showing the effect of perturbations in initial conditions and static disturbance for the controller designed using LQR theory.

Case 3: Initial conditions: perturbed; static disturbance; no dynamic disturbances; improved response

The output responses of the system shown in Figure 5.3 (pole placement design) can be improved by searching for new pole locations which give near optimal response. By a process of trial and error, it was found that the following pole locations -25.0, -26.25 -31.25 -21.87 -27.5, -25.0, -16.25, -13.1, and -11.25 resulted in improved responses. These are shown in Figure 5.5. Also note that the improvement in the outdoor responses was achieved while not exceeding the maximum capacity of the control inputs. In the following cases, the pole locations obtained in this case will be used unless otherwise stated.

Case 4: Initial conditions: perturbed; static and dynamic disturbances

During the heating season, it is reasonable to expect cold days with sunshine. The solar radiations entering the zones through windows are useful heat gains although variable in nature. In order to simulate a cold day with solar heat gain, we consider the following conditions: a step change in initial conditions and outdoor temperature. The magnitudes of these changes remain the same as those used in case 3. Furthermore, consider a step change $w = 0.5\ KW/m^2$ in solar heat gains entering the zones. Under these conditions, the output responses obtained are shown in Figure 5.6 (pole placement design) and Figure 5.7 (LQR design).

As shown in Figure 5.6, all the outputs go to their respective reference values in about 22 minutes. The effect of adding a dynamic disturbance can be seen from the control input curves shown in the same Figure. The control inputs continue to decrease even though the outputs have reached their desired values. The reason

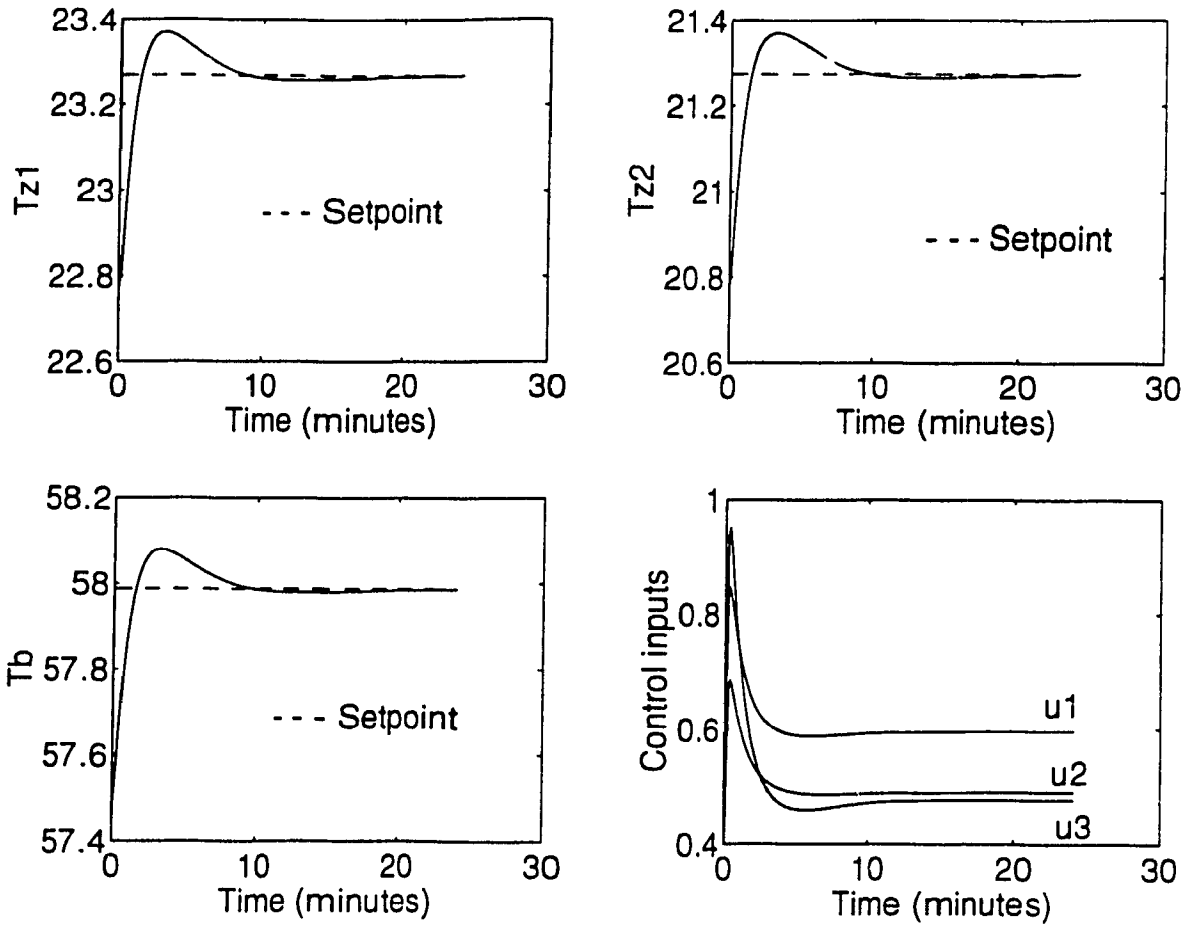

Figure 5.5: Closed-loop response showing the effect of perturbations in initial conditions and static disturbances for the controller designed using pole placement theory: Improved response.

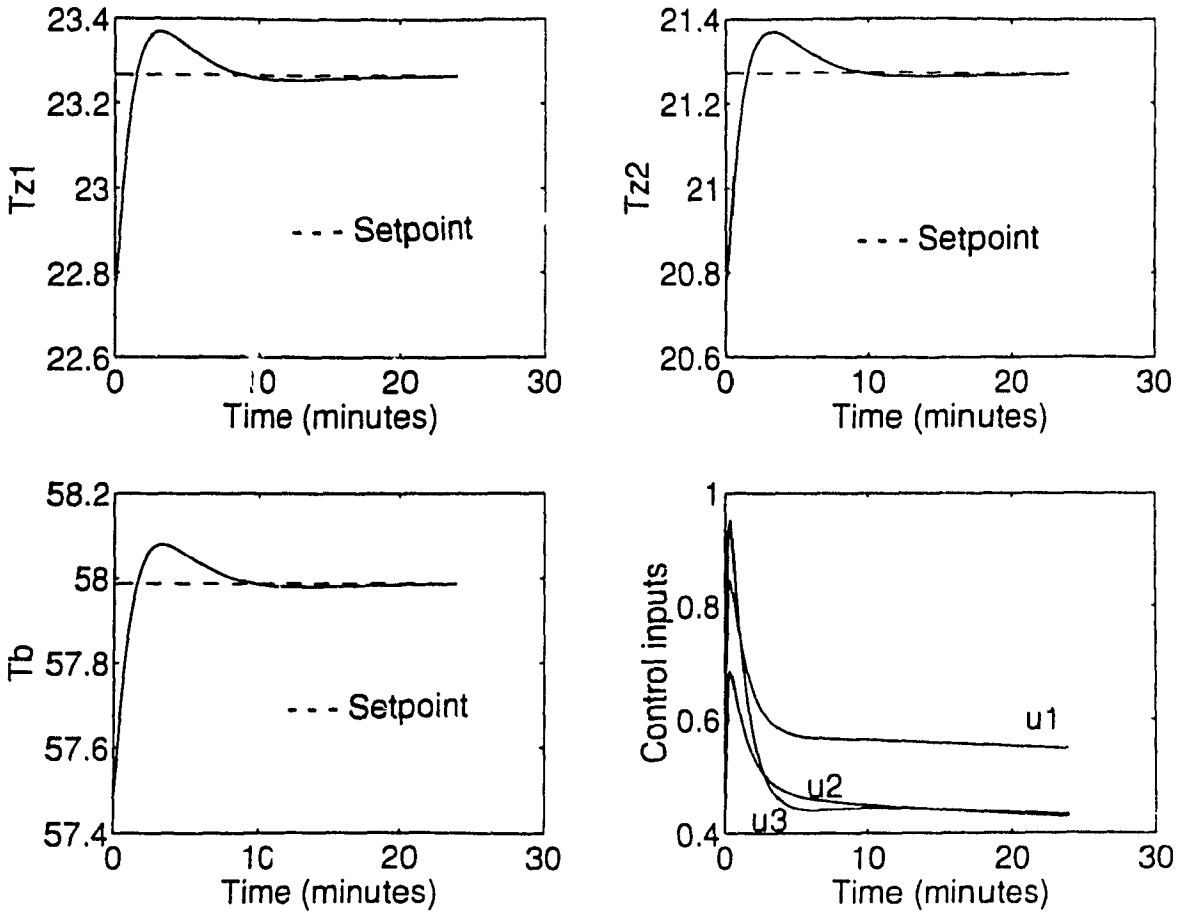

Figure 5.6: Closed-loop response showing the effect of perturbation in initial conditions, static, and dynamic disturbances for the controller designed using pole placement theory

is that since the dynamic disturbance is continuously changing, the controller outputs are also change continuously in order to hold the outputs at their respective setpoints.

Figure 5.7 shows the responses of the closed-loop system obtained with LQR design. It is apparent that the controller is able to regulate the system's outputs to their respective setpoints.

Case 5: Initial conditions: perturbed; dynamic disturbance only

The effect of a step change in the solar heat gain (dynamic disturbance), i.e., $w = 0.5\ KW/m^2$ only, is shown in Figure 5.8 (pole placement design) and Figure 5.9 (LQR design). The initial conditions and the outdoor temperature were held at their respective operating point values.

The effect of solar heat gains on the magnitude of the control inputs can be seen by comparing the magnitudes of the steady-state control inputs in Figure 5.9 and Figure 5.2 (without solar gains). It is apparent that the solar heat gains are useful in that the auxiliary energy required to heat the zones is decreased.

5.3 Robustness

Several parameters of the MFCH system can change during continuous operation. Most importantly, parameters such as the zone heat-loss coefficient and the effectiveness of the fan-coil units are likely to vary by as much as 30 %. To test the controller responses to changes in such system parameters, several simulation runs were carried out. The results are shown in Figures 5.10-5.13 (pole placement design) and Figures 5.14-5.17 (LQR design). These results are compared with those shown

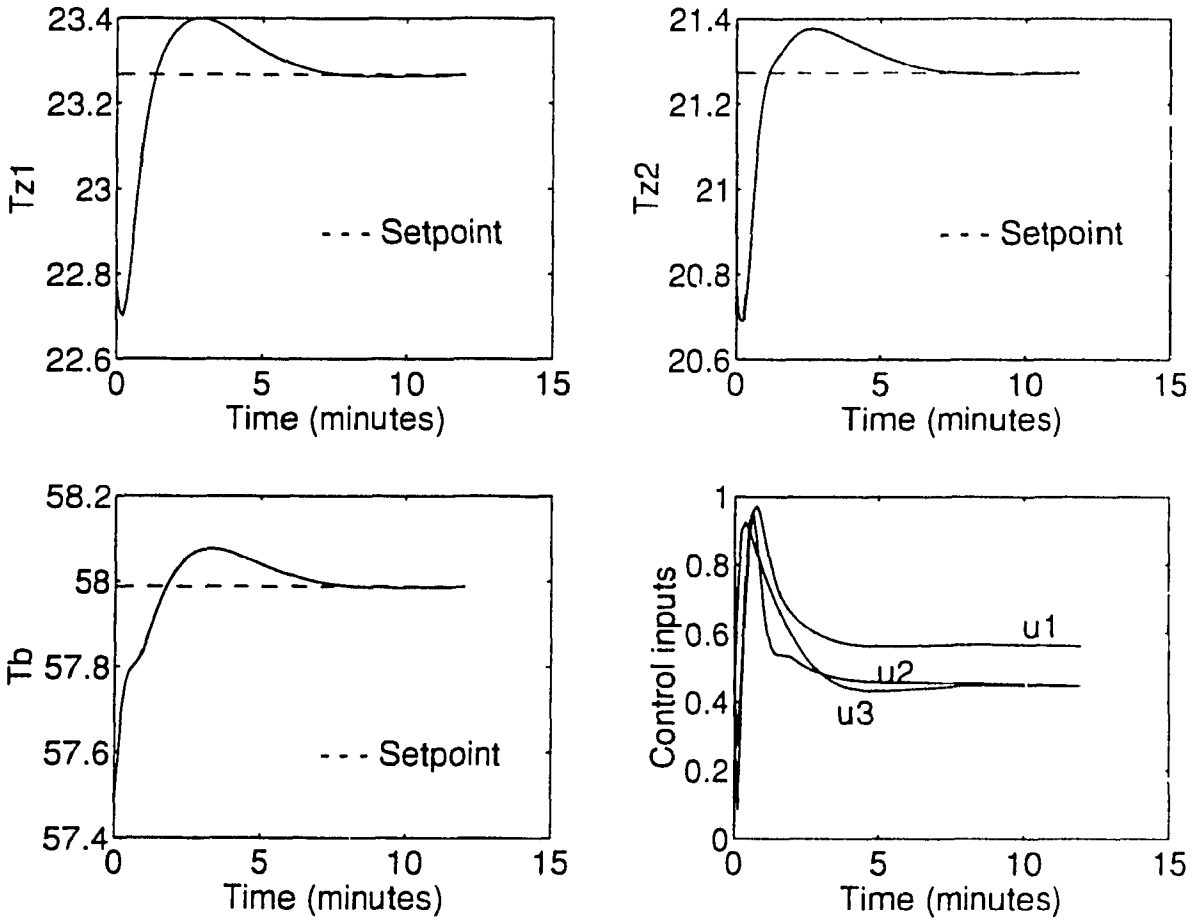

Figure 5.7: Closed-loop response showing the effect of perturbations in initial conditions, static, and dynamic disturbances for the controller designed using LQR theory.

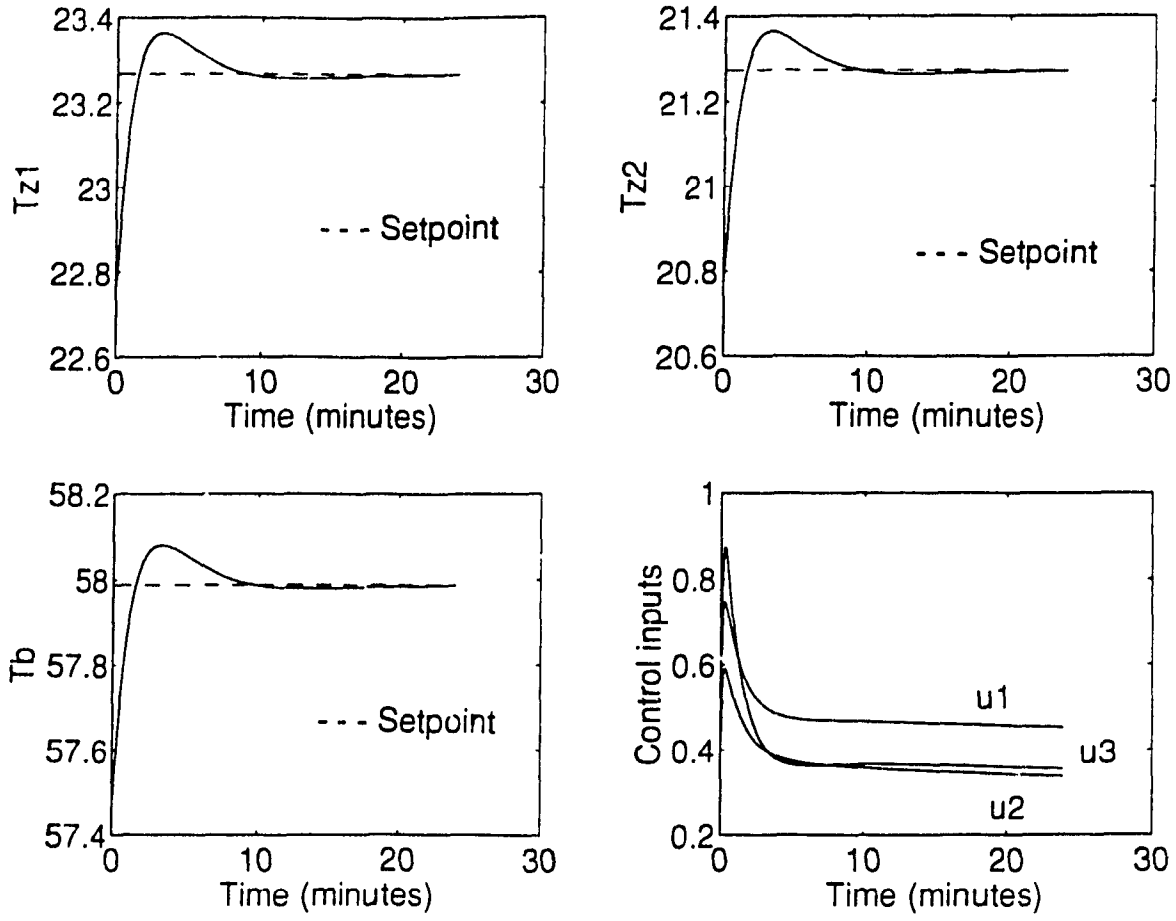

Figure 5.8: Closed-loop response showing the effect of perturbation in initial conditions and dynamic disturbance for the controller designed using pole placement theory

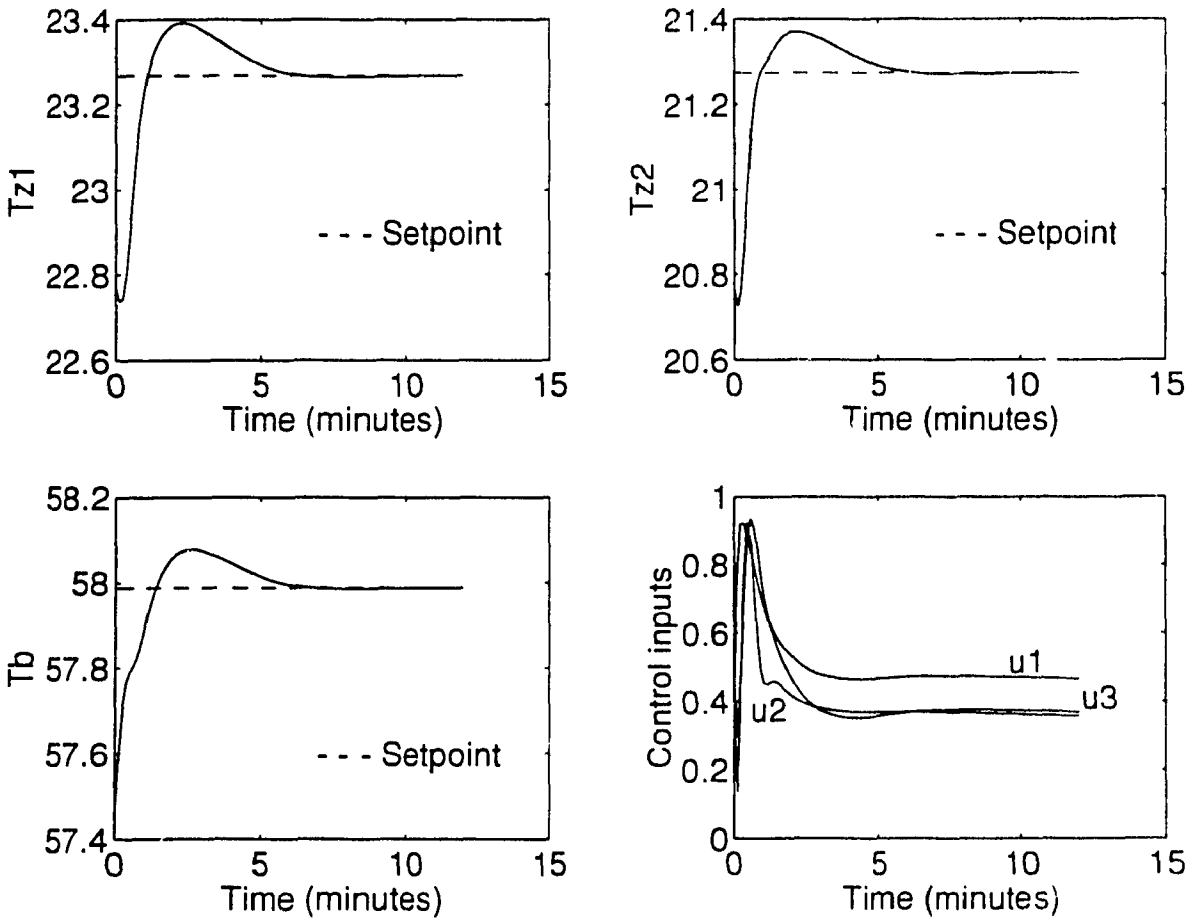

Figure 5.9: Closed-loop response showing the effect of perturbations in initial conditions and dynamic disturbance for the controller designed using LQR theory

in Figure 5.5. The effect of decrease in zone-1 heat loss coefficient a_{z1} by 30 % from its nominal value is shown in Figure 5.10. Only the transient response of zone-1 temperature T_{z1} is affected. The magnitude of the control input u_1 (in steady state) has decreased to cope with this change. All system outputs go to their desired steady state values. The effect of changing the heat loss coefficient of zone-1 and zone-2 i.e. a_{z1}, a_{z2}, by 30 % each, on the output responses are shown in Figure 5.11. On the other hand Figure 5.12 shows the effect of decreasing the effectiveness of the fan-coil unit ξ_z by 20 %. The output responses shown in Figure 5.13 correspond to the case when all three parameters i.e. a_{z1}, a_{z2}, and ξ_z were changed simultaneously by 30 %, 30 %, and 20 % respectively. The results depicted in Figure 5.13 show that the system outputs go to the reference values in spite of the changes in the system parameters. Hence it shows that the controller is robust.

The corresponding sets of results obtained with the LQR design are depicted in Figures 5.14-5.17 The results show that the zone temperatures and the boiler temperature are regulated to their respective setpoints.

5.4 Effect of Introducing Estimation-Error Feedback

Figure 5.18 shows the response of the system when there is no feedback of estimation-error ϵ_s to the controller. The controller was designed using LQR design technique. We use control law given in equation (3.28) as:

$$\Delta \mathbf{u} = -K_1 \Delta \xi - K_2 \Delta \mathbf{x} \tag{5.3}$$

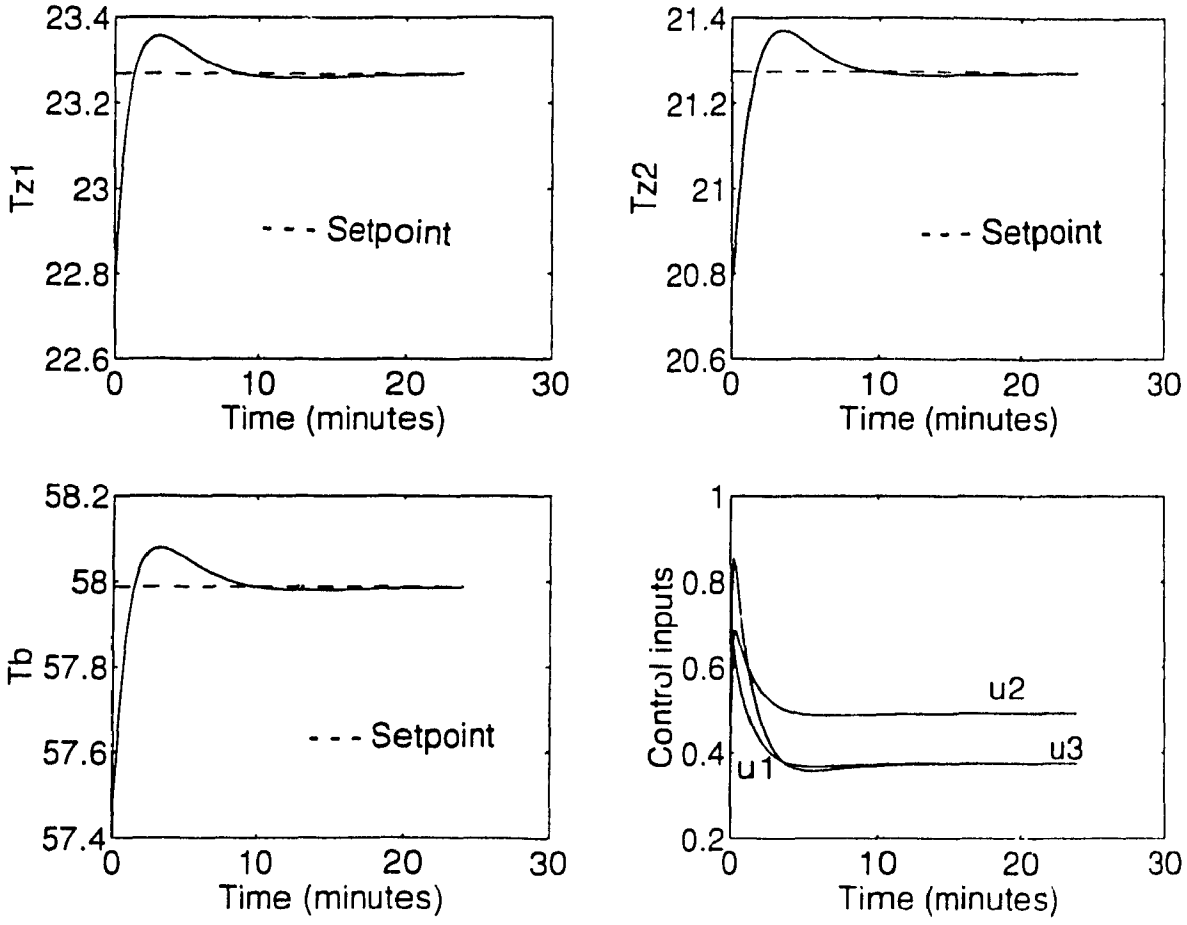

Figure 5.10: Closed-loop response showing the robustness properties when the controller is designed using pole placement theory: a_{s1} is changed by 30 %

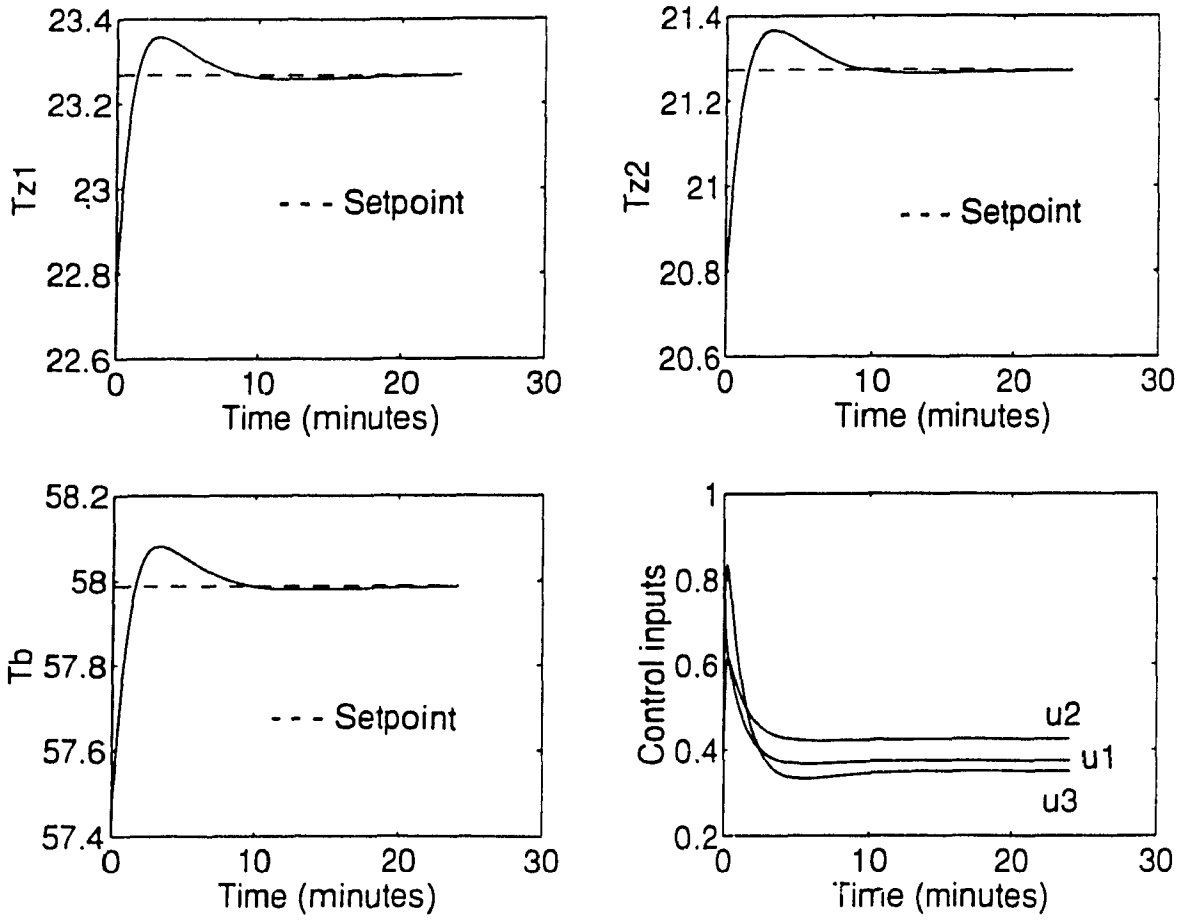

Figure 5.11: Closed-loop response showing the robustness properties when the controller is designed using pole placement theory: a_{z1} and a_{z2} are changed by 30 % each.

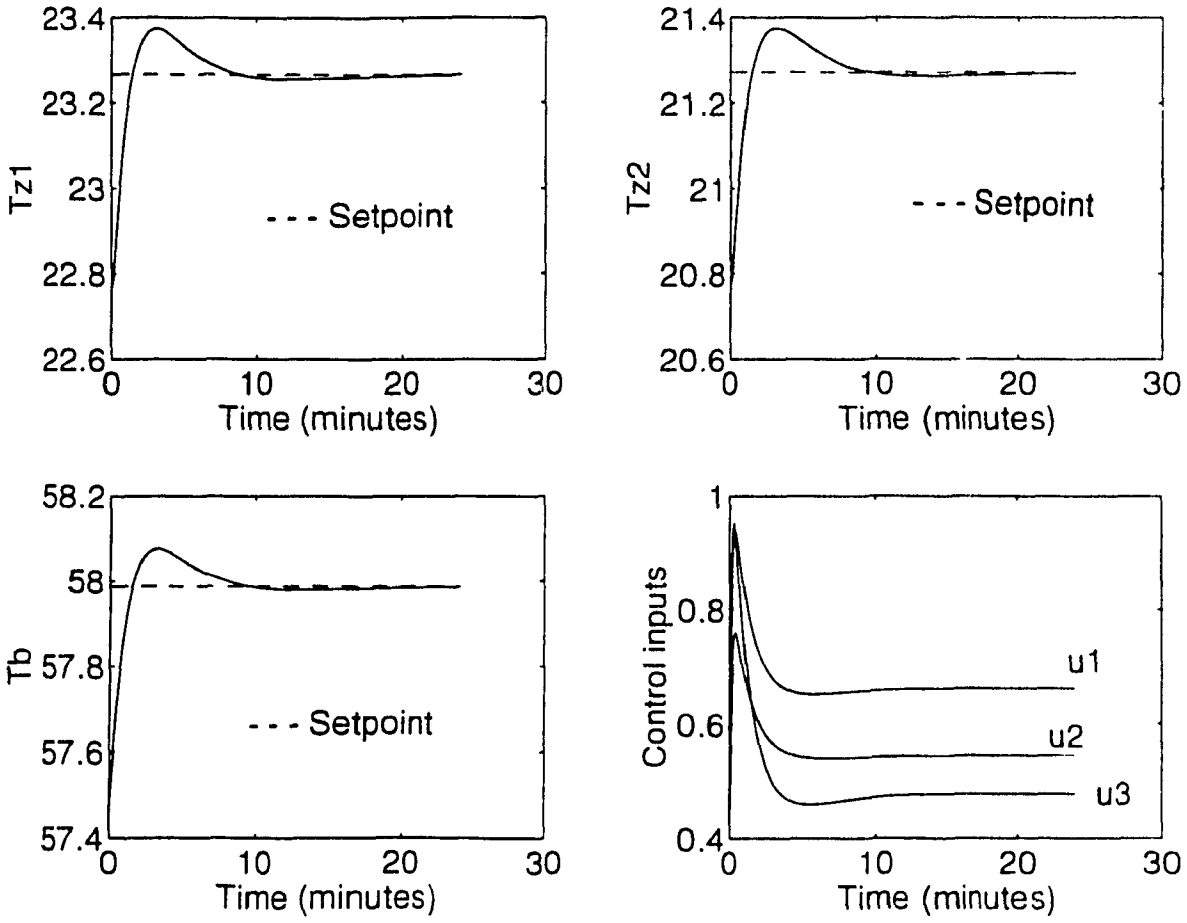

Figure 5.12: Closed-loop response showing the robustness properties when the controller is designed using pole placement theory: ξ_z is changed by 20 %

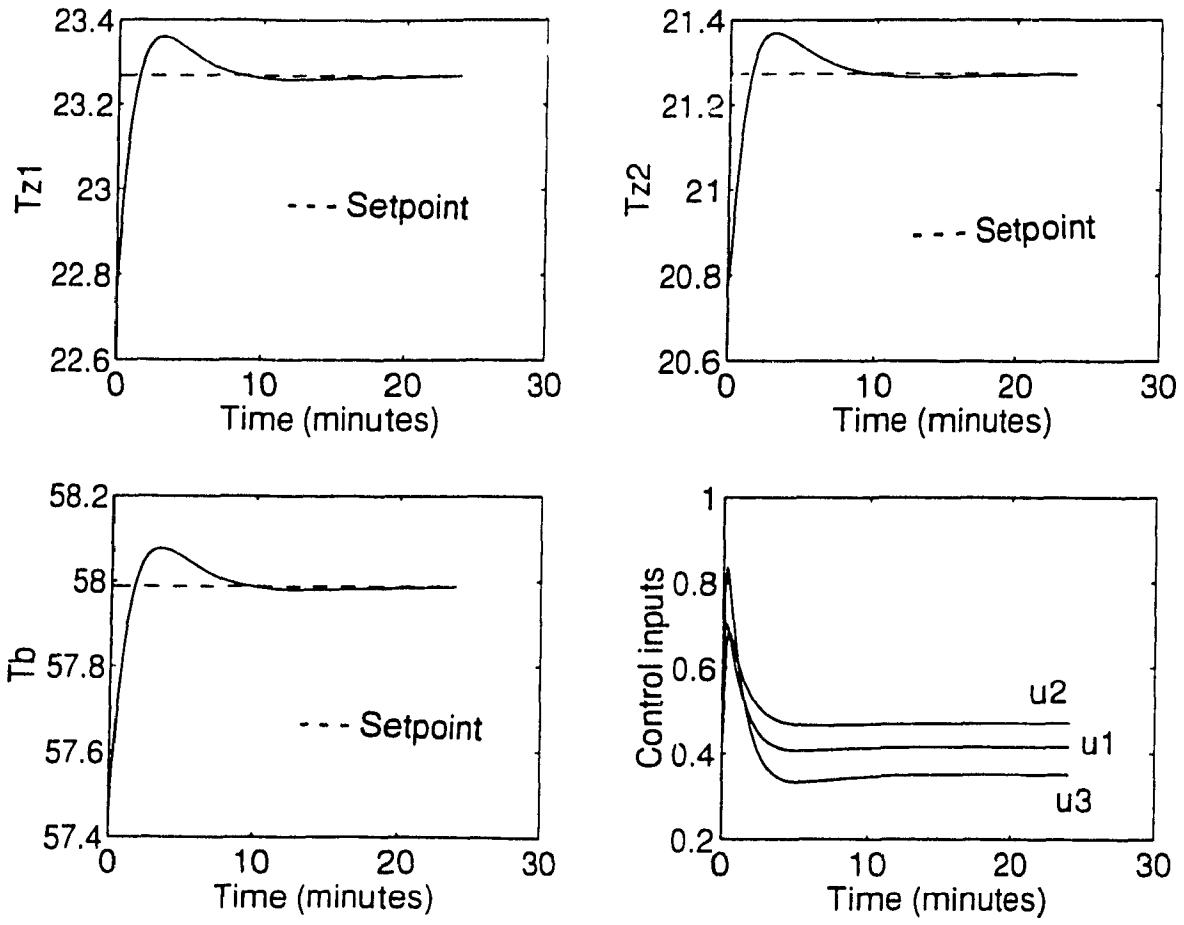

Figure 5.13: Closed-loop response showing the robustness properties when the controller is designed using pole placement theory: a_{z1}, a_{z2}, and ξ_z are changed by 30 %, 30 %, and 20 % respectively.

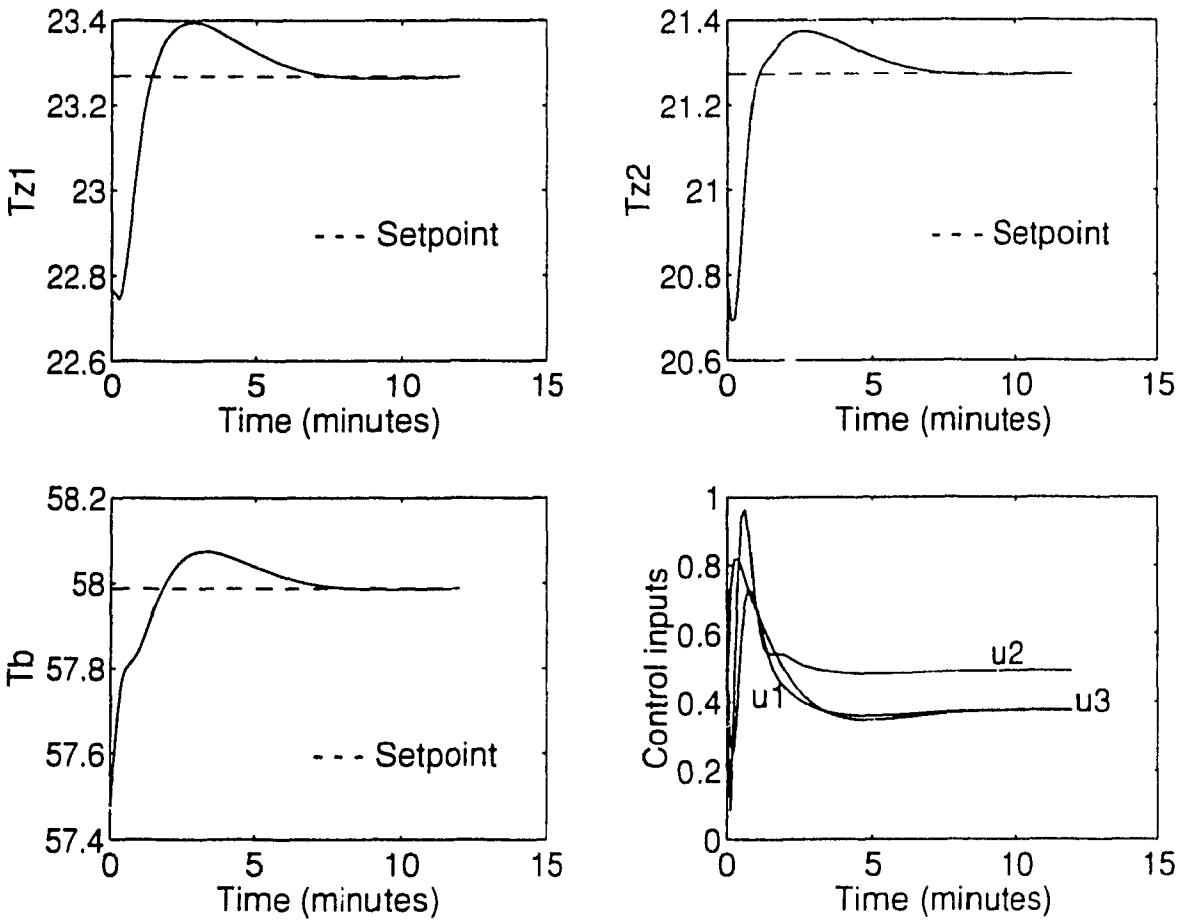

Figure 5.14: Closed-loop response showing the robustness properties when the controller is designed using LQR theory: a_{z1} is changed by 30 %

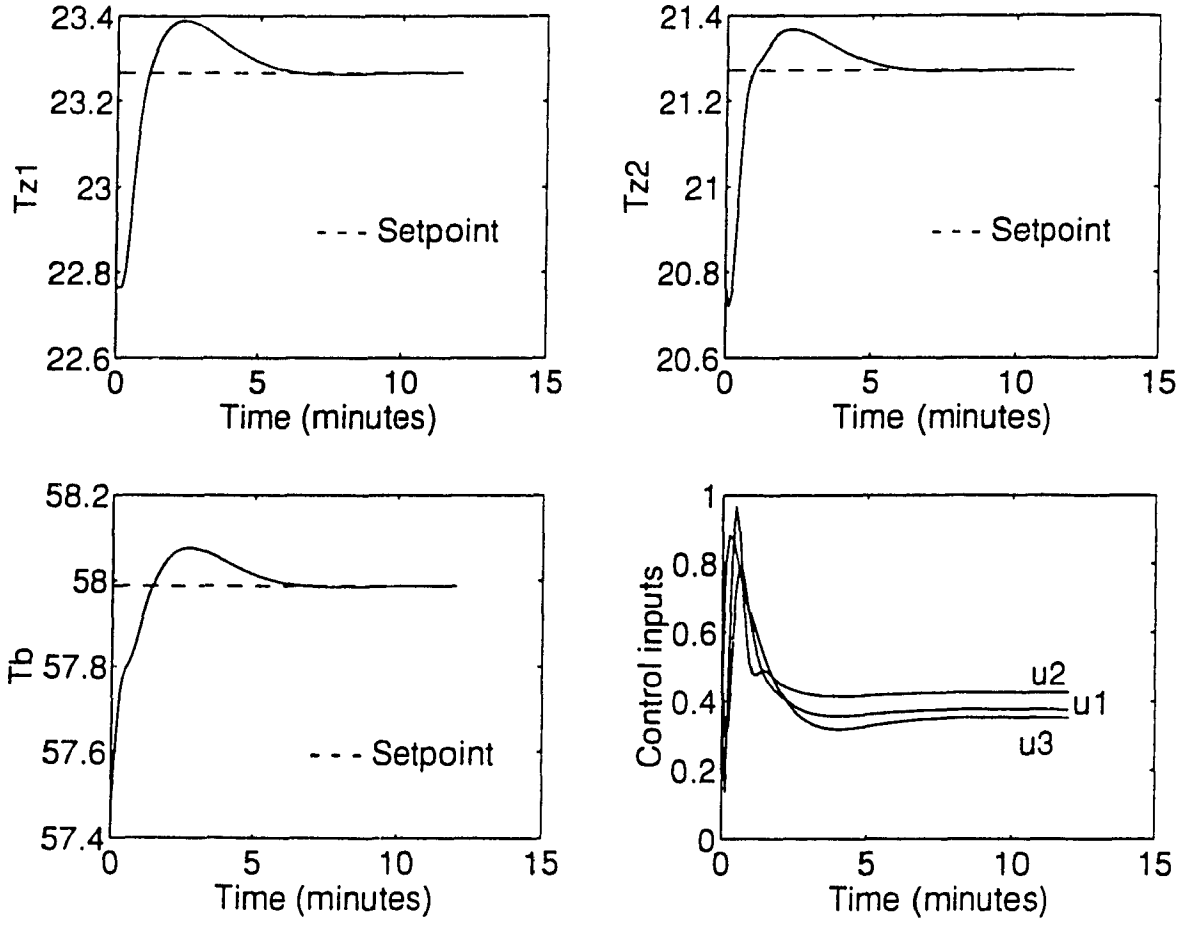

Figure 5.15: Closed-loop response showing the robustness properties when the controller is designed using LQR theory: a_{z1} and a_{z2} are changed by 30 % each.

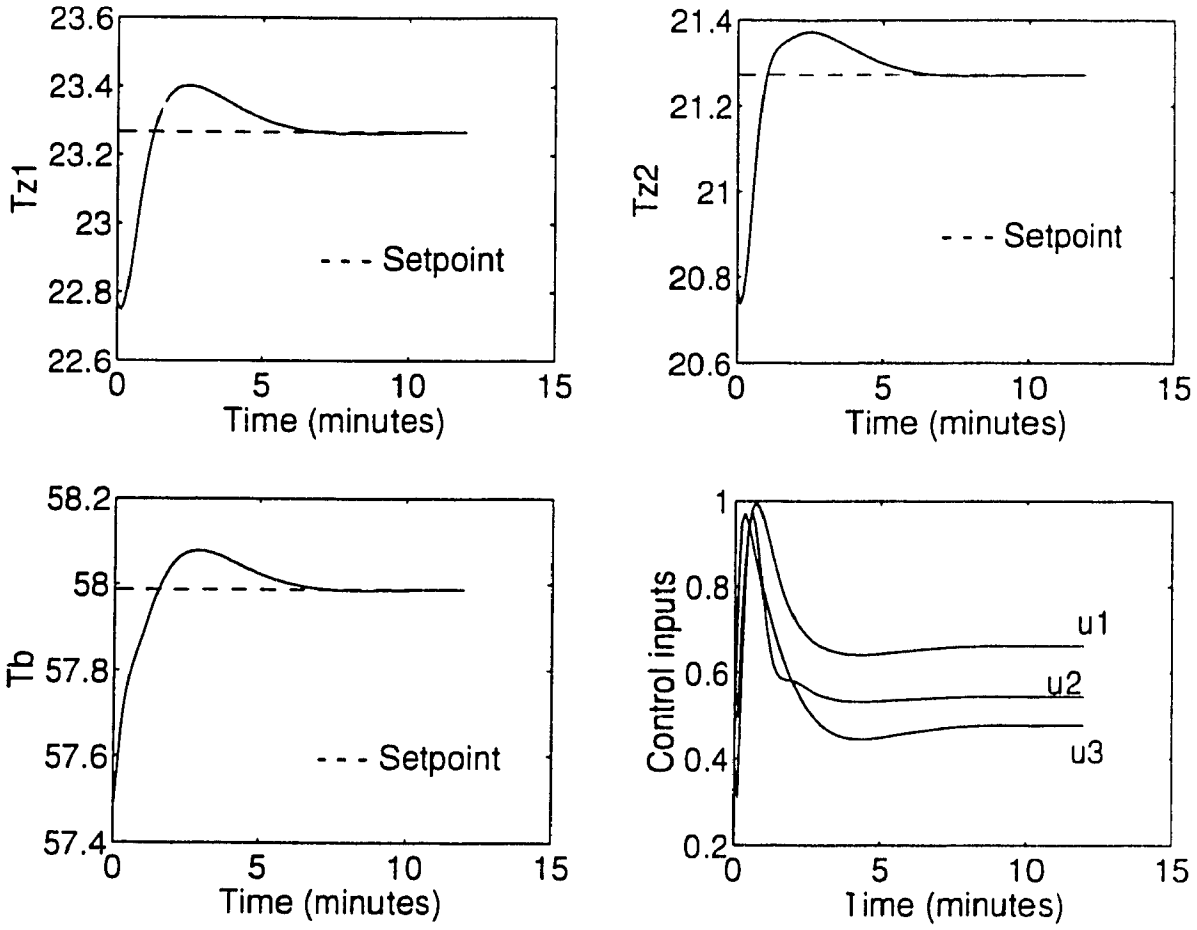

Figure 5.16: Closed-loop response showing the robustness properties when the controller is designed using LQR theory: ξ_z is changed by 20 %.

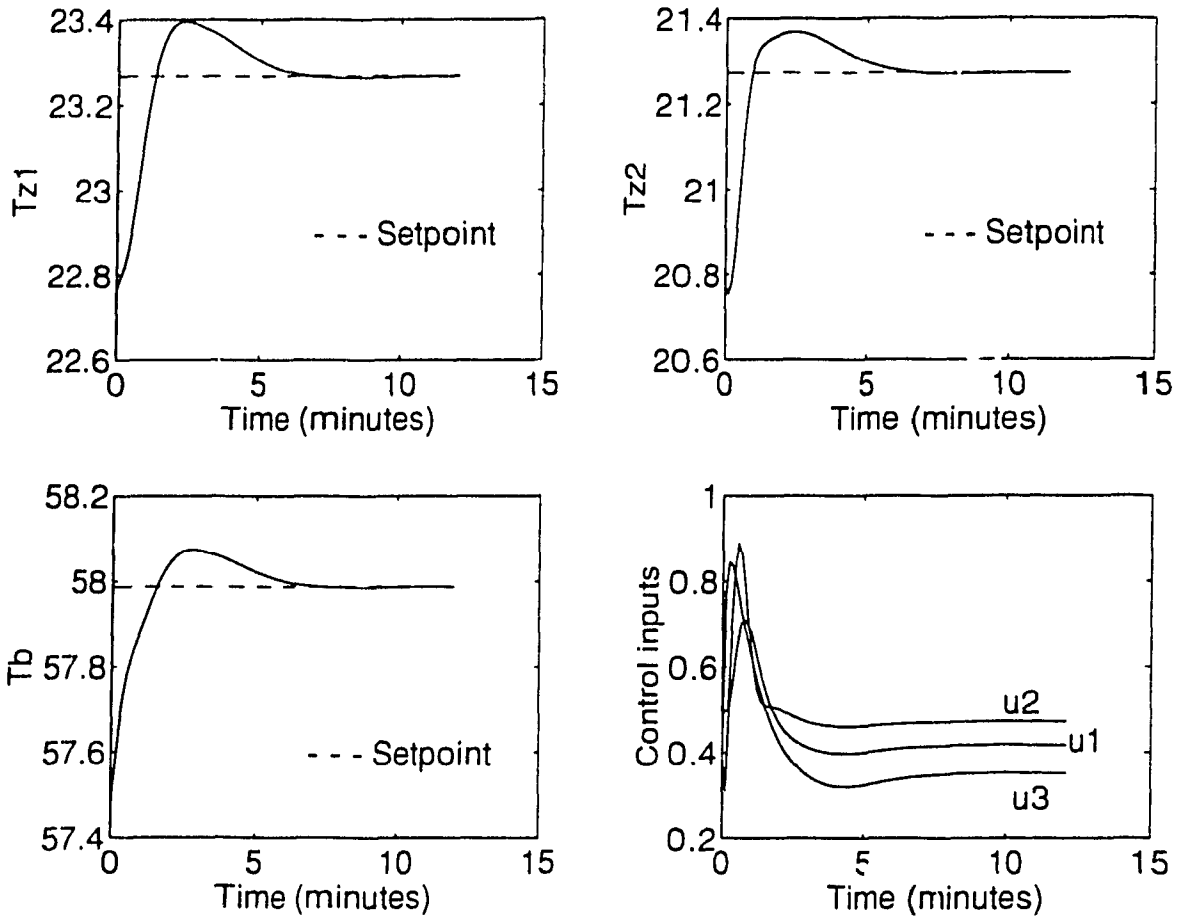

Figure 5.17: Closed-loop response showing the robustness properties when the controller is designed using LQR theory: a_{z1}, a_{z2}, and ξ_z are changed by 30 %, 30 %, and 20 % respectively.

We compare the results shown in Figure 5.18 with Figure 5.4 and it is shown in Figure 5.18 that the response of the system is slower as compared to the system's response in Figure 5.4. Thus a controller takes longer time to cancel the effects of static disturbance acting on the system when there is no feedback of estimation error e_s to the controller.

5.5 Effect of Adding Extra Dynamics

In the model equations (3.4)-(3.6), the characteristics of the control valve are assumed to be linear. In a majority of the cases, the valve lift verses flow rate characteristics are nonlinear. To test how the proposed controller design responds to such nonlinear unmodeled dynamics, we introduced exponential characteristics to describe the control valves. The system equations with exponential valve dynamics in u_1 and u_2 controls are described by the following equations.

$$\begin{aligned}
\frac{dT_{z1}}{dt} &= u_1 C_1 V_1 (T_b - T_{z1}) - C_2(T_{z1} - T_a) - C_3(T_{z1} - T_{z2}) + \\
&\quad f_1(T_{d_{11}} - T_{z1}) \qquad (5.4)\\
\frac{dT_{z2}}{dt} &= u_2 C_4 V_2 (T_b - T_{z2}) - C_5(T_{z2} - T_a) + C_6(T_{z1} - T_{z2}) + \\
&\quad f_2(T_{d_{12}} - T_{z2}) \qquad (5.5)\\
\frac{dT_b}{dt} &= u_3 C_7 (1 - \alpha \frac{T_b}{T_{b_{max}}}) - C_8(T_b - T_p) - u_1 C_9(T_b - T_{z1}) - \\
&\quad u_2 C_{10}(T_b - T_{z2}) \qquad (5.6)
\end{aligned}$$

where $V_1 = 1 - e^{-\beta u_1}$, $V_2 = 1 - e^{-\beta u_2}$ and $\beta = 5$.

The output responses of the system with nonlinear valve dynamics are shown in Figure 5.19 (pole placement design) and Figure 5.20 (LQR Design). It is apparent that the addition of exponential valve dynamics to the actual plant does not affect

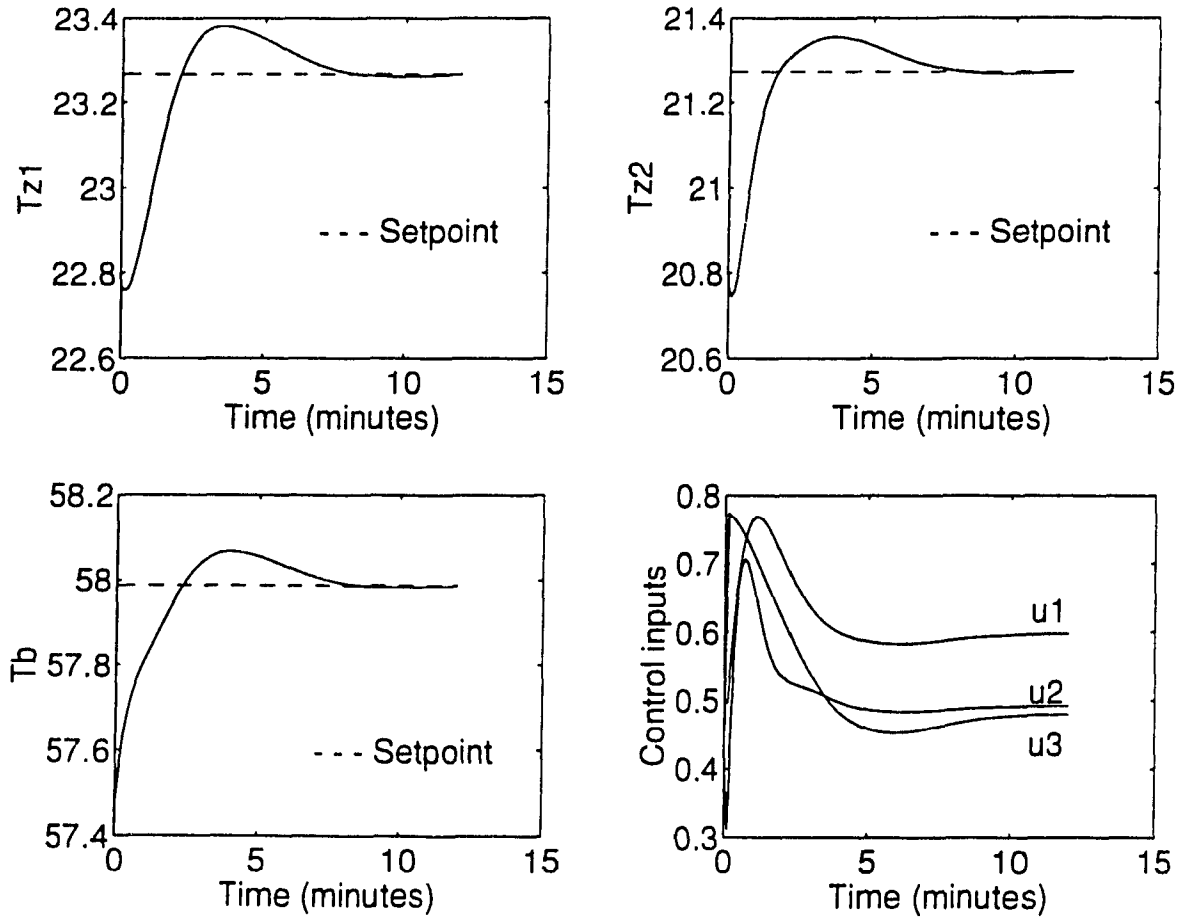

Figure 5.18: Closed-loop response when there is no estimation-error feedback to the controller.

the performance of the closed-loop system. The output responses are smooth and good regulation of the zone temperatures and the boiler temperature is achieved

5.6 Comparison of Adaptive Controller with Fixed-Gain Controller

Usually the zone temperature setpoints in buildings are setback during unoccupied hours and setforward during occupied hours. The magnitude of this change is usually between $3-5$ deg C. In order to simulate this case, we considered a 3 deg C change in the operating point of the system. How the system with adaptive controller reacts to these changes is depicted in Figure 5.21. All the outputs go to their desired steady-state values while control inputs remain bounded between 0 and 1. Figure 5.22 shows the response of the system with fixed controller, i.e. matrices K_1 and K_2 were non-varying, to the step changes in the operating point. It is shown in Figure 5.22 that all the outputs do not go to their desired steady-state values. Thus it shows that the implementation of the adaptive controller to the MFCH system provides better response while keeping all the control inputs with in bounds, i.e. between 0 and 1. The results shown in Figure 5.21 and Figure 5.22 were obtained when the controller was designed using pole placement theory.

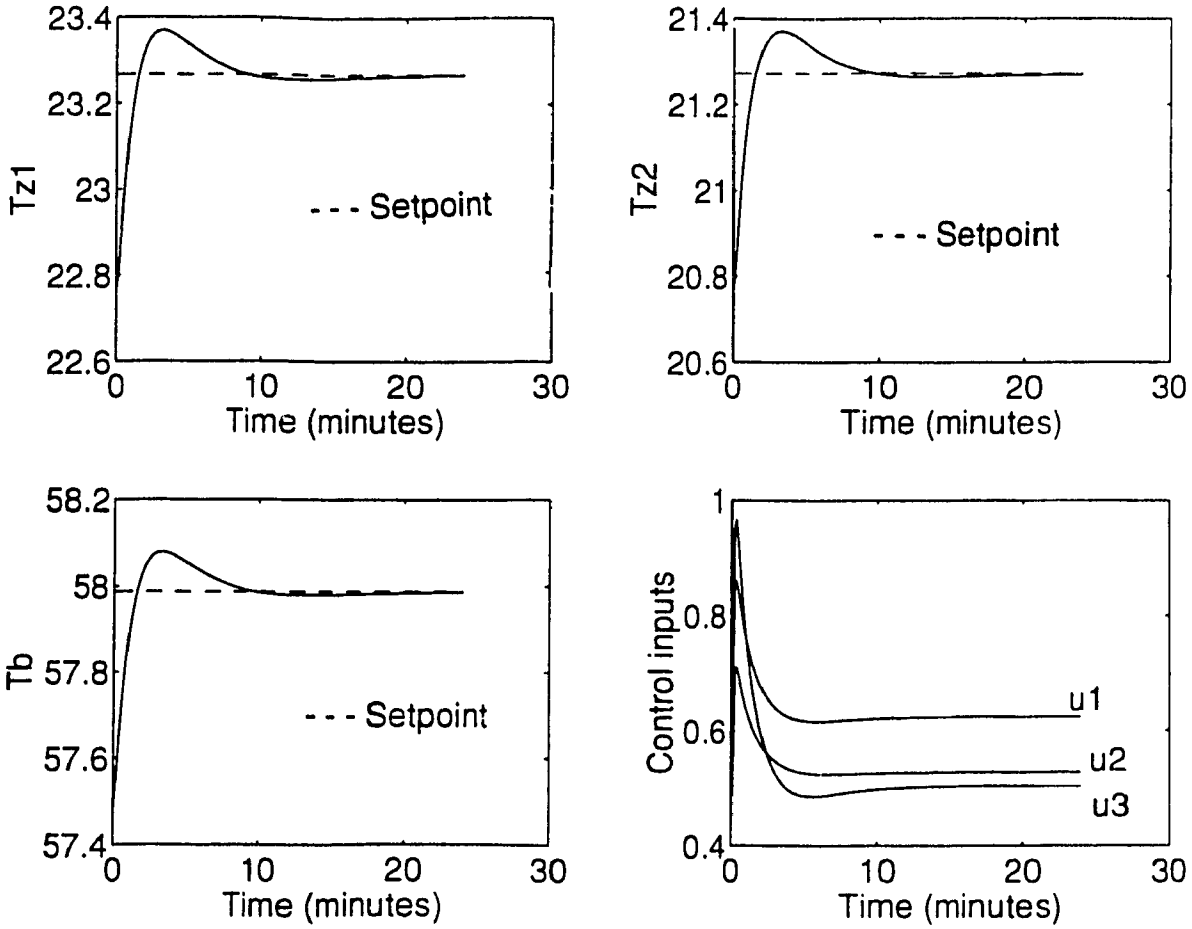

Figure 5.19: Closed-loop response showing the effect of adding extra valve dynamics when the controller is designed using pole placement.

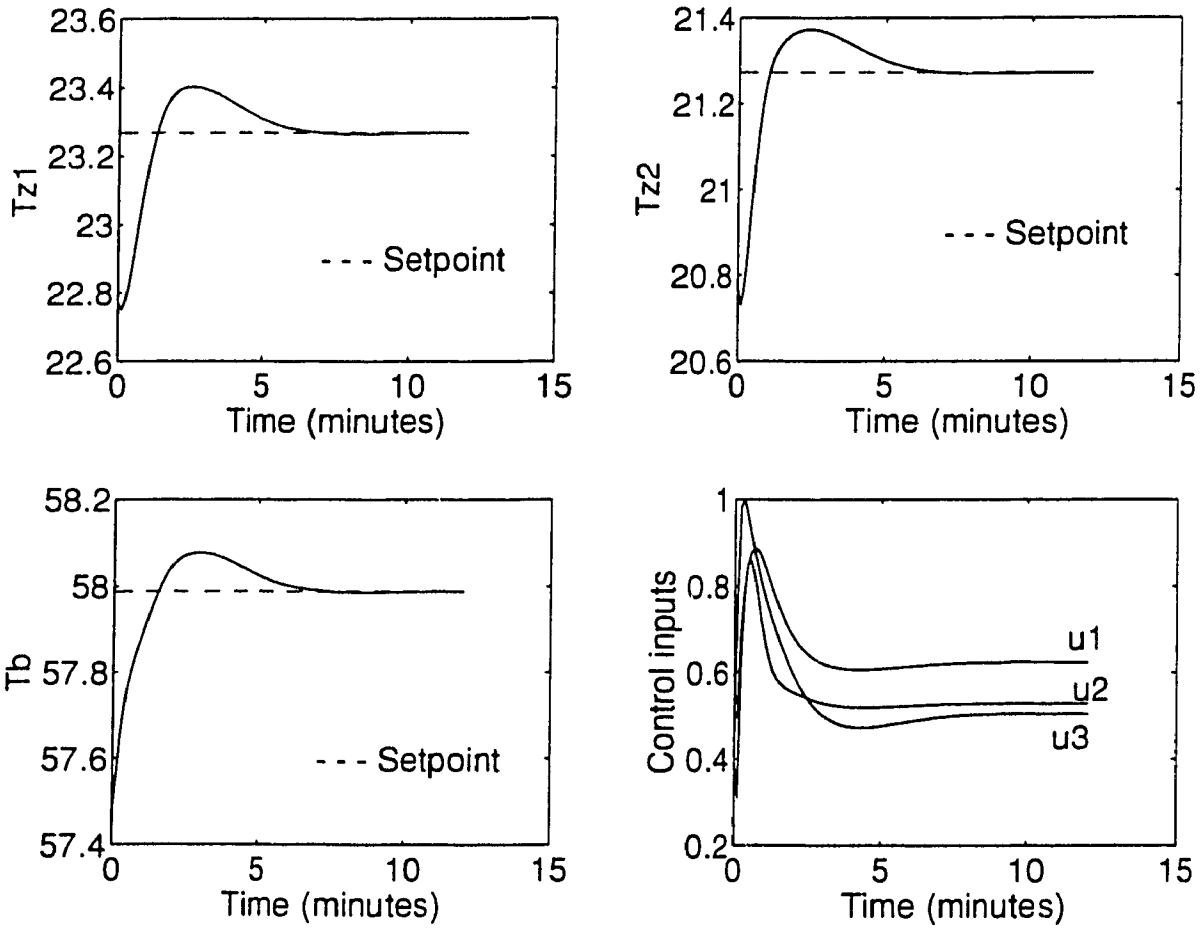

Figure 5.20: Closed-loop response showing the effect of adding extra valve dynamics when the controller is designed using LQR.

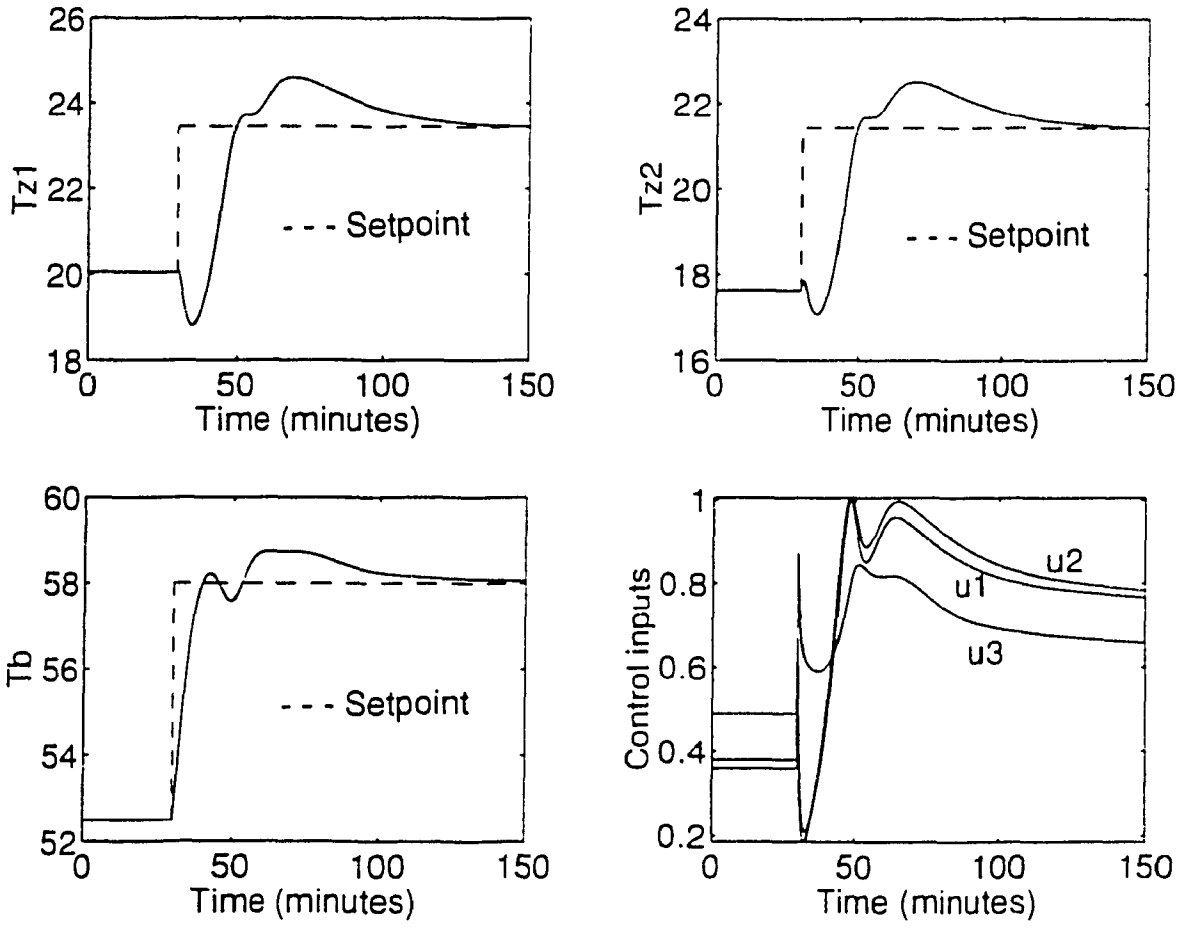

Figure 5.21: Closed-loop response showing the effect of step changes in the operating point with adaptive controller.

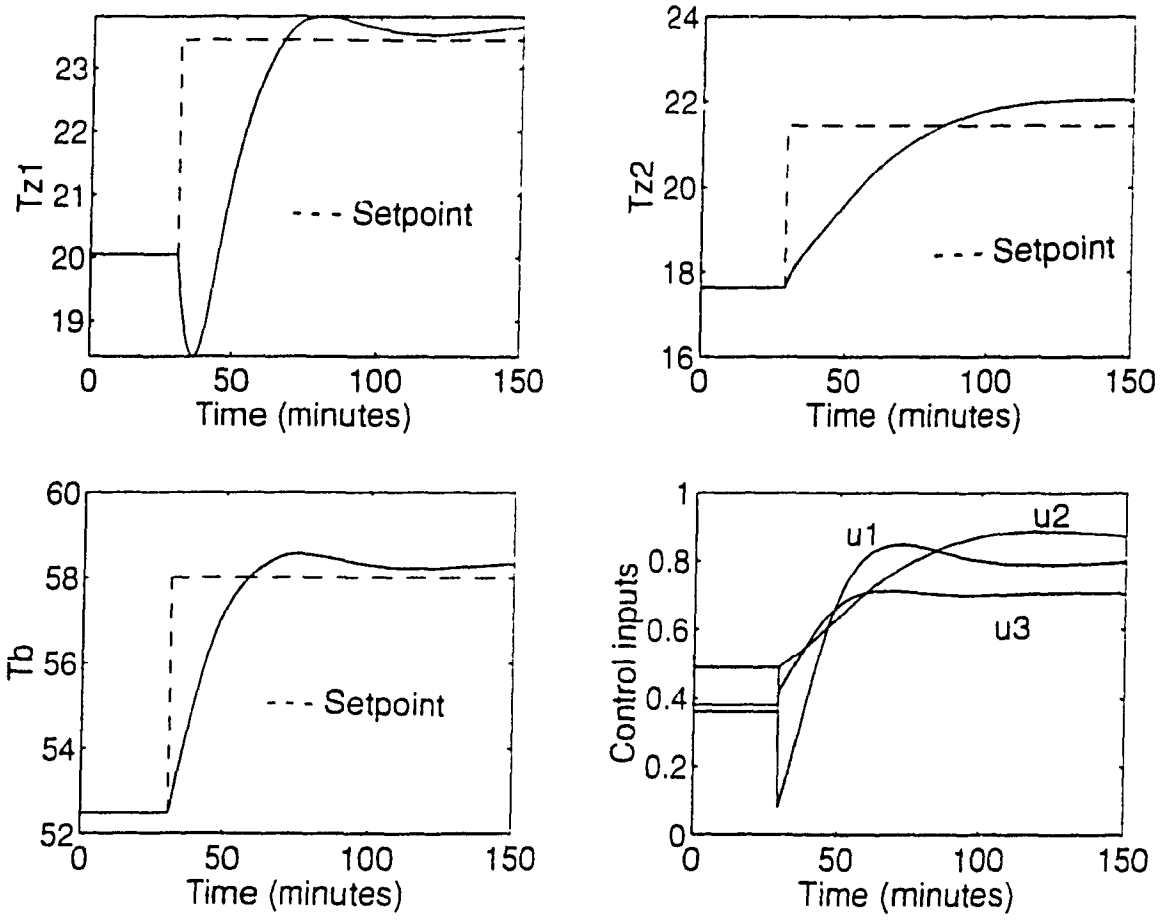

Figure 5.22: Closed-loop response showing the effect of step changes in the operating point with fixed-gain controller.

Chapter 6

Conclusions and Extensions

The adaptive control methods examined in HVAC applications are limited to single-input/single-output systems. Another problem is that in practice, the HVAC systems, which are MIMO systems, are tuned by considering one controller at a time. This leads to severe controller interaction problems. In this thesis, we have considered a three-input/three-output MFCH system and shown how an adaptive controller can be designed for such systems which include both robust and tracking properties.

From the results obtained from the adaptive control implementation of a robust servomechanism controller on a given MFCH system, the following conclusions can be drawn.

1. The simulation results show that the designed adaptive controller is stable under a wide range of operating conditions and changes in the system parameters.

2. It has been shown that the closed-loop system is stable for all operating conditions as long as $K_3 = \hat{B}^{-1}$, and K_1 and K_2 are obtained using pole placement

or LQR theory.

3. The simulation results show that controller is able to reject the effects of both static and dynamic disturbances rapidly.

Some specific conclusions about the performance of the closed-loop system with the designed controller are follows:

1. The effect of a step change of $-5.0\,\mathrm{deg}\,C$ in outdoor temperature, T_a, was rejected in less than 10 minutes.

2. The controller is able to restore the system from one operating condition to another (a $3\,\mathrm{deg}\,C$ step change) in about 100 minutes.

3. The maximum percentage overshoot in zone temperatures was found to be 0.52 %, which is well within acceptable limits.

4. Tests for robustness show that changes in system parameters a_{z1}, a_{z2}, and ξ_z by 30 %, 30 %, and 20 % respectively, from their nominal values did not effect the performance of the closed-loop system.

5. The controller is able to adapt to extra or more accurate/complex valve dynamics of exponential form.

The work described in this thesis can be extended further in the following way:

1. Experimental work is needed to validate the control system design.

2. A better approach should be developed to obtain the desired set of pole locations (when pole placement theory is used) e.g. from input-output data, or by conducting open-loop tests.

3. While computing matrices Q and R, the constraints on control input could be given.

4. Comparison with other adaptive control approaches, e.g. adaptive pole placement, model reference adaptive control etc. could be done.

References

1. K. J. Astrom. "Theory and Applications of Adaptive Control-A Survey", *Automatica*. Vol. 19, No. 5, pp. 471-486, 1983.

2. K. S. Narendra and Y. H. Lin. "Design of stable model reference adaptive controllers", *Applications of Adaptive Control*, edited by K. S. Narendra and R. V. Monopoli. Academic Press, New York, 1980.

3. R. F. Drenick and R. A. Shabender, "Adaptive servomechanism", *AIEE Transactions*, Vol. 76, pp. 286-292. Nov. 1957.

4. K. Ogata. *Modern Control Engineering*. Prentice-Hall. Englewood Cliffs, N.J., 1970.

5. J. A. Aseltine, A. R. Mancini. and C. W. Sarture, "A survey of adaptive control systems". *IRE Transactions on Automatic Control*. Vol. 3, pp. 102-108, Dec. 1958.

6. V. W. Eveleigh. *Adaptive Control and Optimization Techniques*. McGraw-Hill, New York, 1967.

7. M. Margolis and C. T. Leondes, "A parameter tracking servo for adaptive control systems", *IRE Transactions on Automatic Control*, Vol. 4, pp. 100-111, Nov. 1959.

8. L. A. Zadeh, "On the definition of adaptivity", *Proceedings of IEEE*, Vol. 51, pp. 569-570, March 1963.

9. D. M. Schwenk, "Single-loop digital controllers in HVAC", *ASHRAE Transactions*, Vol. 94, pp. 1985-1994, Part 2, 1988.

10. S. Boonyatikarn and J. R. Jones, "Smart Building Control Strategies: Research and Application", *ASHRAE Technical Data Bulletin*, Vol. 5, No. 5

11. *ASHRAE handbook-HVAC systems and applications*, pp. 51.1-51.4, American Society of Heating, Refrigerating, and Air-Conditioning Engineers, Inc., Atlanta, GA, 1987.

12. Y. H. Chen, K. M. Lee, and W. J. Wepfer, "Adaptive robust control scheme applied to a single-zone HVAC system", *Proc. of American Control Conference*, pp. 1076-1081, May 1990.

13. J. W. MacArthur, E. W. Grald and A. F. Konar, "An effective approach for dynamically compensated adaptive control", *ASHRAE Transactions*, pp. 415-423, Vol. 95, Part 2, 1989.

14. C. J. Harris and S. A. Billings, "Self-tuning and adaptive control: Theory and applications", Peter Peregrinus, New York, 1981.

15. K. J. Astrom and T. Hagglund, "Automatic tuning of simple regulators with specifications on phase and amplitude margins", *Automatica*, Vol. 20, No. 5,

pp. 645-651, 1984.

16. C. G. Nesler, "Adaptive Control of Thermal Processes in Buildings", *IEEE Control Systems Magazine*, pp. 9-13, August 1986.

17. A. O. Wallonborg, "A New Self-Tuning Controller for HVAC Systems", *ASHRAE Transactions*, Vol. 97, Part 1, pp. 19-25, 1991.

18. M. J. Pinnella, E. Wechselberger, D. C. Hittle, and C. O. Pedersen, "Self-Tuning Digital Integral Control", *ASHRAE Transactions*, Part 2B, Vol. 92, pp. 202-210, 1986.

19. C. G. Nesler, "Automated Controller Tuning For HVAC Applications", *ASHRAE Transactions*, Part 2B, Vol. 92, pp. 189-201, 1986.

20. M. A. Townsend, D. B. Cherchas, and A. Abdelmessih, "Optimal Control of a General Environmental Space", *Transactions of the ASME*, Vol. 108, pp. 330-339, December 1986.

21. P. S. Curtiss, J. F. Kreider, and M. J. Brandemuehl "Adaptive Control of HVAC Processes Using Predictive Neural Networks", *ASHRAE Transactions*, Vol. 99, pp. 496-504, Part 1, 1993.

22. A. L. Dexter, "Self-Tuning Optimum Start Control of Heating Plant", *Automatica*, Vol. 17, No. 3, pp. 483-492, 1981.

23. S. G. Brandt, "Adaptive Control Implementation Issues", *ASHRAE Transactions*, Vol.92, Part 2B, pp. 211-219, 1986.

24. Y. Nishikawa, N. Sannomiya, T. Ohta, and H. Tanaka, "A method for auto tuning of PID control parameters", *Automatica*, Vol. 20, No. 3, pp. 321-332, 1984.

25. J. E. Bekker, P. H. Meckl, and D. C. Hittle, "A tuning method for first-order process with PI controllers", *ASHRAE Transactions*, Vol. 97, Part 2, pp. 19-23, 1991.

26. F. G. Jota and A. L. Dexter, "Self-tuning control of an air-handling plant", *Proc. Control 88*, IEE Conf. Pub. No. 285, pp. 41-46, 1988.

27. W. J. Graham and A. L. Dexter, "Self-tuning control of the heating plant in a large building", *Proc. of Int. Conf. Control 85*, IEE Publ. No. 252, 2, Cambridge, UK, 575-580.

28. *ASHRAE Handbook of Fundamentals*, American Society of Heating, Refrigerating, and Air-Conditioning Engineers, Atlanta, GA, 1993.

29. M. Zaheer-uddin and R. V. Patel, "Optimal tracking control of multizone indoor environment spaces", submitted to *ASME J. of Dyn. Syst. Meas. and Control*, 1993.

30. G. F. Franklin, J. D. Powell, *Digital Control of Dynamic Systems*, Addison-Wesley, Reading, MA, 1980.

31. K. J. Astrom, B. Wittenmark, *Computer Controlled Systems*, Prentice-Hall, Englewood Cliffs, N.J. 1984.

32. E. J. Davison and A. Goldberg, "Robust control of a general servomechanism problem: the servo compensator", *Automatica*, Vol. 11, pp. 461-471, 1975.

33. R. V. Patel and N. Munro, *Multivariable System Theory and Design*, Pergamon Press, Oxford, England, 1982.

34. R. V. Patel and P. Misra, "Numerical algorithm for eigenvalues assignment by state feedback", *Proc. IEEE*, pp. 1755-1764, 1984.

35. P. Misra, *Computational Methods for Multivariable System Analysis and Design*, Ph.D dissertation, Dept. Elect. & Comput. Engr., Concordia University, Canada, 1987.

36. H. Seraji, "Design of pole-placement compensators for multivariable systems", *Automatica*, Vol. 16, pp. 335-338, 1980.

37. G. S. Miminis and C. C. Paige, "An algorithm for pole-assignment of time-invarient linear system", *Int. J. Contrl.*, Vol. 35, pp. 341-354, 1982.

38. F. Fallside Ed., *Control System Design by Pole-Zero Assignment*, Academic Press, London, 1977.

39. L. Ljung and T. Soderstrom, "Theory and practice of recursive identification", MIT Press, Cambridge, MA, 1983.

40. K. J. Astrom and B. Wittenmark, *Adaptive Control*, Addison-Wesley, Reading, MA, 1989.

41. E. J. Davison, "The robust control of a servomechanism problem for linear time-invariant multivariable systems", *IEEE Transactions on Automatic Control*, Vol. AC-21, pp. 25-34, 1976.

42. K. S. Narendra and A. Annaswamy, *Stable Adaptive Systems*, Prentice Hall, Englewood Cliffs, NJ, 1989.

43. B. A. Francis, "The multivariable servomechanism problem from the input output point of view", *IEEE Transactions on Automatic Control*, Vol. AC-22, pp. 322-328, 1977.

44. T. Kailath, *Linear Systems*, Prentice-Hall, Englewood Cliffs, N.J., 1980.

45. B. D. O. Anderson and J. B. Moore, *Linear Optimal Control*, Prentice Hall, Englewood Cliffs, 1971.

46. I. J. Nagrath and M. Gopal, *Control System Engineering*, Wiley Eastern Ltd., Bombay, India, 1982.

47. W. A. Coppel, "Stability and asymptotic behavior of differential equations", Boston, Heath Mathematical Monographs, 1965.

48. W. Hahn, "Theory and applications of Lyapunov's direct method", Prentice-Hall, Englewood Cliffs, NJ, 1963.

49. J. P. LaSalle and S. Lefschetz, "Stability by Liapunov's direct method", Academic Press, New York 1961.